

Supporting Information

Far-red fluorescence and chiroptical properties of pyrrolopyrrole aza-BODIPYs induced by the B,O-chelation

Shuhei Fukami,^a Shigeki Mori,^b Takunori Harada^c and Soji Shimizu^{*a}

^aDepartment of Applied Chemistry, Graduate School of Engineering and Centre for Molecular Systems, Kyushu University, Fukuoka 819-0395, Japan

^bAdvanced Research Support Centre (ADRES), Ehime University, Matsuyama 790-8577, Japan

^cDepartment of Integrated Science and Technology, Faculty of Science and Technology, Oita University, Oita 870-1192, Japan

Contents:

- i. Experimental
- ii. HR-MS Spectra
- iii. NMR Spectra
- iv. Crystallographic Data
- v. UV/vis Absorption, Excitation and Fluorescence Spectra
- vi. Electrochemistry
- vii. DFT and TDDFT Calculations
- viii. Estimation of Dissymmetry Factors of Theoretical CD and CPL
- ix. References
- x. Appendix

i. Experimental

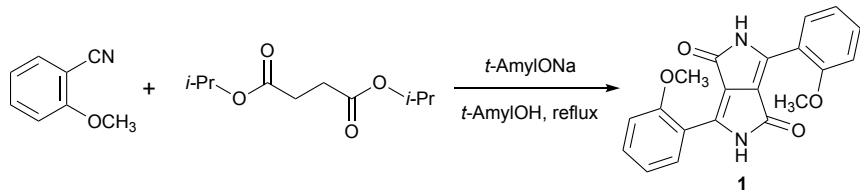
General procedure: High-resolution mass spectrometry was performed on a BRUKER micrOTOF-Q III spectrometer (ESI mode with Tuning Mix as an external standard calibration). ¹H NMR spectra were recorded on a JEOL JNM-ECX500R spectrometer (operating at 495.132 MHz for ¹H, 124.501 MHz for ¹³C and 465.8894 MHz for ¹⁹F) using residual solvent as an internal reference for ¹H (δ = 7.26 ppm for CDCl₃ and δ = 5.32 ppm for CD₂Cl₂) and ¹³C (δ = 77.16 ppm for CDCl₃) and using trifluoroacetic acid as an external reference for ¹⁹F (δ = -76.55 ppm). Electronic absorption spectra were recorded on a JASCO V-770 spectrophotometer. Fluorescence spectra in solution were measured on a JASCO FR-8650 spectrometer. Absolute fluorescence quantum yields in solution were measured on a HAMAMATSU C13534-21 calibrated integrating-sphere system with self-absorption correction. Circular dichroism (CD) spectra were measured on a JASCO J-1500 spectrophotometer. Circularly polarized luminescence (CPL) and DC (= nonpolarized fluorescence) spectra were measured on a Comprehensive Chiroptical Spectrophotometer (CCS-1)¹ equipped with the Stokes-Mueller matrix analysis system. The excitation wavelength was set to be 620 nm, and the emission spectra were recorded over a wavelength range of 850–650 nm with 980 V high-tension voltage, 33 mm slit width and 10 nm spectral bandwidth for the excitation and emission monochromators. The CPL dissymmetry factors (g_{CPL}) were calculated according to $g_{\text{CPL}} = \Delta F (= I_L - I_R)/F (= I_L + I_R)$, where I_L and I_R are the intensities of the left- and right-handed CPL emissions.² Preparative separations were performed using silica gel column chromatography (KANTO Silica Gel 60 N, spherical, neutral, 40–50 μm or KANTO Silica Gel 60 N, spherical, neutral, 63–210 μm). Thin-layer chromatography (TLC) was performed with aluminum sheet silica gel 60 F₂₅₄ (Merck). All reagents and solvents used for syntheses were of commercial reagent grade and were used without further purification except where noted. Spectroscopic grade solvents were used for spectroscopy.

Crystallographic data collection and structure refinement: Suitable crystals for X-ray diffraction analysis were obtained by a vapor diffusion method. Data collection was carried out at -173 °C on a Rigaku Saturn724 diffractometer with MoK α radiation. The structure was solved by a direct method (SHELXT)³ and refined using a full-matrix least squares technique (SHELXL).⁴ CCDC 2342651 and 2343541 contain the supplementary crystallographic data for this paper. These data can be obtained free of charge via www.ccdc.cam.ac.uk/data_request/cif, or by emailing data_request@ccdc.cam.ac.uk, or by contacting The Cambridge Crystallographic Data Centre, 12 Union Road, Cambridge CB2 1EZ, UK; fax: +44 1223 336033.

Electrochemical measurements: Cyclic voltammograms (CV) were recorded on a CH Instrument Model 620B (ALS) under an argon atmosphere in an *o*-dichlorobenzene (*o*-DCB) solution with 0.1 M tetra-*n*-butylammonium perchlorate (TBAP) as a supporting electrolyte. Measurements were made with a glassy carbon working electrode, a Ag/AgCl reference electrode and a Pt wire counter electrode. The concentration of the solution was fixed at 0.5 mM, and the scan rates were set to 100 mV s⁻¹ for CV measurements. A ferrocenium/ferrocene (Fc⁺/Fc) couple was used as an internal standard.

Theoretical calculation details: The Gaussian 16 software package⁵ was used to perform DFT and TDDFT calculations using the ω B97XD⁶ with 6-31G(d) basis set.⁷

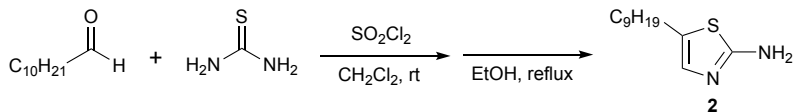
Synthetic procedure



Scheme S1. Synthesis of 3,6-bis(2-methoxyphenyl)-2,5-dihydropyrrolo[3,4-c]pyrrole-1,4-dione (**1**).

3,6-Bis(2-methoxyphenyl)-2,5-dihydropyrrolo[3,4-c]pyrrole-1,4-dione (1**):** **1** was synthesized according to the literature procedure with slight modifications.⁸ Sodium (1.5 g, 65 mmol) and a small amount of iron(III) chloride were added to dry *t*-amyl alcohol (25 mL), and the mixture was refluxed. After sodium was dissolved, 2-methoxybenzonitrile (3.8 mL, 30 mmol) was added. Diisopropyl succinate (3.0 mL, 15 mmol) was added dropwise to the reaction mixture over 20 h. After completion of the addition, the reaction mixture was allowed to cool to room temperature, and acetic acid (32 mL) and methanol (50 mL) were added. The precipitate was filtered and washed with methanol and water to afford **1** as a dark red solid (235 mg, 4.5%).

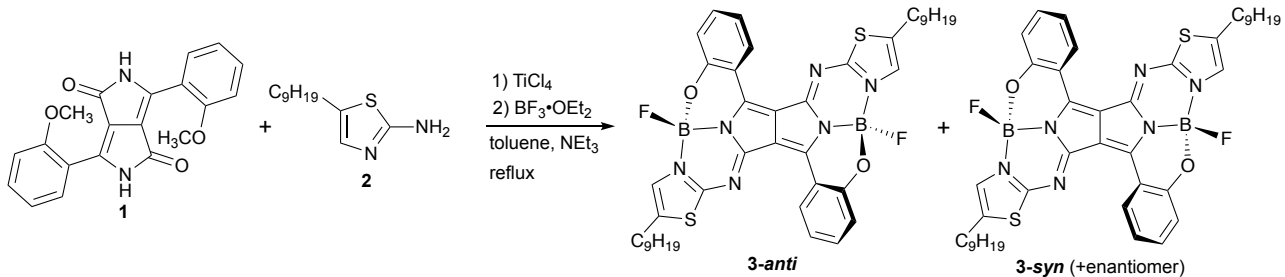
¹H NMR (495 MHz, CD₂Cl₂ and one drop of D₂O, 297 K): δ [ppm] 9.34 (br, 2H), 9.21 (d, J = 8.0 Hz 2H), 7.51 (t, J = 15.1 Hz, 2H), 7.20 (t, J = 15.5 Hz, 2H), 7.07 (d, J = 8.5 Hz, 2H), 4.79 (s, 6H).



Scheme S2. Synthesis of 2-amino-5-nonylthiazole (**2**).

2-Amino-5-nonylthiazole (2**):** **2** was synthesized according to the literature procedure with slight modifications.⁹ 1-Undecanal (6.9 mL, 36 mmol) and thiourea (4.5 g, 1.6 eq) were suspended in dry dichloromethane (15 mL). The mixture was cooled to 0 °C, and SO₂Cl₂ (3.0 mL, 1.2 eq) was added dropwise. Then the mixture was allowed to warm up to 15–25 °C. After stirring for 2 h, most of the solvent was removed under reduced pressure, and dry ethanol (15 mL) was added. The mixture was refluxed for 4 h. The solvent was evaporated, water was added, and the crude mixture was extracted with ethyl acetate and washed with aqueous NaHCO₃ solution. After drying over Na₂SO₄ and evaporation of the solvent, the mixture was purified by silica gel column chromatography (CH₂Cl₂/MeOH = 20:1 (v/v)) to give **2** as a white solid (4.2 g, 51%).

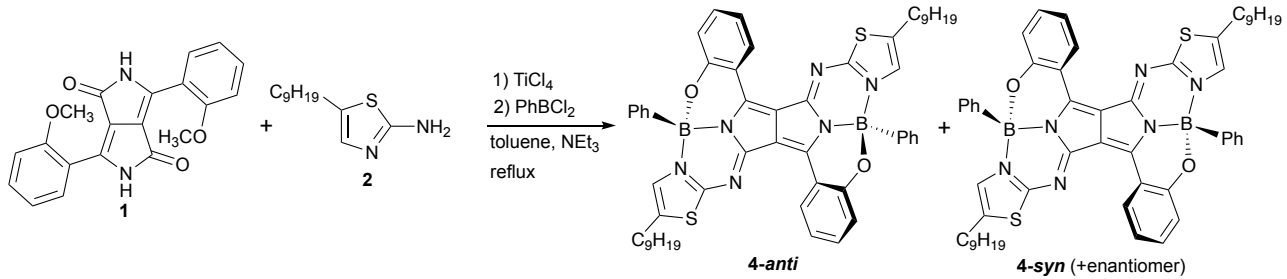
¹H NMR (495 MHz, CDCl₃, 297 K): δ [ppm] 6.72 (s, 1H), 4.71 (br, 2H), 2.62 (t, J = 7.7 Hz, 2H), 1.29–1.17 (m, 14H), 0.87 (t, J = 7.0 Hz, 3H).



Scheme S3. Synthesis of *B,O*-chelated PPAB with fluorine ligands (**3**).

B,O-Chelated PPAB with fluorine ligands (3**):** **1** (62 mg, 0.18 mmol) and **2** (203 mg, 5 eq) were added to dry

toluene (6 mL), and the mixture was refluxed. TiCl_4 (0.11 mL, 6.1 eq) and triethylamine (0.36 mL, 14 eq) were successively added. After 3 h, imine formation was confirmed by TLC analysis, and $\text{BF}_3\cdot\text{OEt}_2$ (0.33 mL, 15 eq) was added. After refluxing overnight, the reaction mixture was poured into water and extracted with dichloromethane. The reaction mixture was dried over Na_2SO_4 , and the solvent was removed by a rotary evaporator. The crude mixture was purified by silica gel column chromatography (CH_2Cl_2 , then $\text{CH}_2\text{Cl}_2/\text{hexane} = 1:3$ (v/v)) to provide **3** as a green solid.

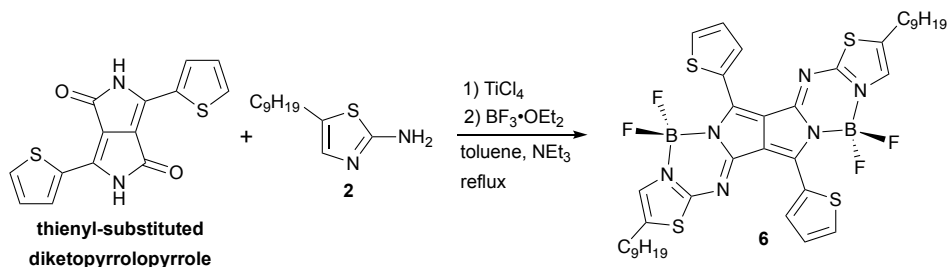


Scheme S4. Synthesis of *B,O*-chelated PPAB with phenyl ligands (**4**).

B,O-Chelated PPAB with phenyl ligands (4): **1** (62 mg, 0.18 mmol) and **2** (203 mg, 5 eq) were added to dry toluene (6 mL), and the mixture was refluxed. TiCl_4 (0.11 mL, 6.1 eq) and triethylamine (0.36 mL, 14 eq) were successively added. After 3 h, the imine formation was confirmed by TLC analysis, and dichlorophenylborane (0.33 mL, 15 eq) was added. After refluxing overnight, the reaction mixture was poured into water and extracted with dichloromethane. The reaction mixture was dried over Na_2SO_4 , and the solvent was removed by a rotary evaporator. The crude mixture was purified by silica gel column chromatography (CH_2Cl_2 , then $\text{CH}_2\text{Cl}_2/\text{hexane} = 1:3$ (v/v)) to provide **4-anti** and **4-syn** as green solids (**4-anti**: 22.3 mg (14%), **4-syn**: 18.9 mg (12%)).

4-anti: ^1H NMR (495 MHz, CD_2Cl_2 , 297 K): δ [ppm] 8.53 (d, $J = 6.5$ Hz, 2H), 7.47 (t, $J = 15.0$ Hz, 2H), 7.26–7.24 (m, 6H), 7.18 (d, $J = 7.5$ Hz, 2H), 7.13–7.06 (m, 8H), 2.71 (td, $J_1 = 7.2$ Hz, $J_2 = 3.4$ Hz, 4H), 1.65 (m, 4H), 1.30–1.26 (m, 24H), 0.88 (t, $J = 6.8$ Hz, 6H); ^{13}C NMR (125 MHz, CDCl_3 , 297 K): δ [ppm] 171.0, 158.4, 151.3, 144.3, 135.0, 132.6, 131.3, 131.0, 127.7, 127.5, 125.8, 120.8, 120.1, 117.9, 114.4, 32.0, 30.5, 29.6, 29.4, 29.4, 29.1, 27.8, 22.8, 14.3; UV-vis (CH_2Cl_2): λ_{\max} [nm] (ϵ [$\text{M}^{-1}\text{cm}^{-1}$]) 349 (32400), 473 (10900), 629 (44200), 689 (157000); HR-MS (ESI): $[\text{M}+\text{H}]^+$ Calcd for $\text{C}_{54}\text{H}_{59}\text{B}_2\text{N}_6\text{O}_2\text{S}_2$: 909.4339; Found: 909.4392 (error: +5.8 ppm).

4-syn: ^1H NMR (495 MHz, CD_2Cl_2 , 297 K): δ [ppm] 8.48 (d, $J = 8.0$ Hz, 2H), 7.47 (t, $J = 16.0$ Hz, 2H), 7.33 (d, $J = 7.75$ Hz, 4H), 7.18–7.11 (m, 10H), 7.07 (t, $J = 15.0$ Hz, 2H), 2.69 (t, $J = 15.8$ Hz, 4H), 1.64 (t, $J = 15.0$ Hz, 4H), 1.33–1.26 (m, 24H), 0.88 (t, $J = 13.5$ Hz, 6H); ^{13}C NMR (125 MHz, CDCl_3 , 297 K): δ [ppm] 171.1, 158.6, 151.0, 144.1, 135.1, 132.6, 131.5, 131.1, 127.8, 127.6, 125.9, 120.7, 119.9, 117.4, 114.1, 32.0, 30.5, 29.5, 29.4, 29.4, 29.1, 27.8, 22.8, 14.3; UV-vis (CH_2Cl_2): λ_{\max} [nm] (ϵ [$\text{M}^{-1}\text{cm}^{-1}$]) 349 (33800), 471 (11000), 624 (46500), 683 (166000); HR-MS (ESI): $[\text{M}+\text{Na}]^+$ Calcd for $\text{C}_{54}\text{H}_{58}\text{B}_2\text{N}_6\text{O}_2\text{S}_2\text{Na}$: 931.4158; Found: 931.4219 (error: +6.5 ppm).



Scheme S5. Synthesis of PPAB with thienyl substituents (**6**).

6: Thienyl-substituted diketopyrrolopyrrole (198 mg, 0.66 mmol) and **2** (678 mg, 5 eq) were added to dry toluene (15 mL), and the mixture was refluxed. TiCl₄ (0.45 mL) and triethylamine (1.3 mL) were successively added. After 3 h, the imine formation was confirmed by a TLC analysis. Then, BF₃·OEt₂ (1.3 mL) was added. After refluxing overnight, the reaction mixture was poured into water and extracted with dichloromethane. The reaction mixture was dried over Na₂SO₄, and the solvent was removed by a rotary evaporator. The crude mixture was purified by silica gel column chromatography (CH₂Cl₂, then CH₂Cl₂/hexane = 1:3 (v/v)) to afford **6** as a green solid (60 mg, 11%).

¹H NMR (495 MHz, CDCl₃, 297 K): δ [ppm] 8.95 (d, J = 4.0 Hz, 2H), 7.76 (dd, J_1 = 5.1 Hz, J_2 = 1.1 Hz, 2H), 7.27 (d, J = 5.1 Hz, 2H), 7.20 (s, 2H), 2.74 (t, J = 7.4 Hz, 4H), 1.71-1.65 (m, 4H), 1.40 (t, J = 7.4 Hz, 4H), 1.27 (s, 20H), 0.88 (t, J = 7.1 Hz, 6H); ¹³C NMR (125 MHz, CDCl₃, 297 K): δ [ppm] 169.6, 152.9, 144.5, 137.5, 133.9, 133.4, 131.5, 128.0, 125.7, 32.0, 30.6, 29.6, 29.4, 29.1, 27.8, 22.8, 14.3; ¹⁹F NMR (465 MHz, CDCl₃, 295 K): δ [ppm] -130.6 (q, J_{B-F} = 30 Hz); UV-vis (CH₂Cl₂): λ_{max} [nm] (ϵ [M⁻¹cm⁻¹]) 341 (46000), 434 (29000), 617 (48000), 675 (117000); HR-MS (ESI): [M+Na]⁺ Calcd for C₃₈H₄₆B₂N₆S₄Na: 835.2694; Found: 835.2755 (error: +7.3 ppm).

ii. HR-MS Spectra

Acquisition Parameters

Source Type	ESI	Ion Polarity	Positive	Set Nebulizer	0.3 Bar
Focus	Not active	Set Capillary	4500 V	Set Dry Heater	180 °C
Scan Begin	100 m/z	Set End Plate	-400 V	Set Dry Gas	4.0 l/min
Scan End	3000 m/z	Offset collision	650.0 Vpp	Set Divert Valve	Source

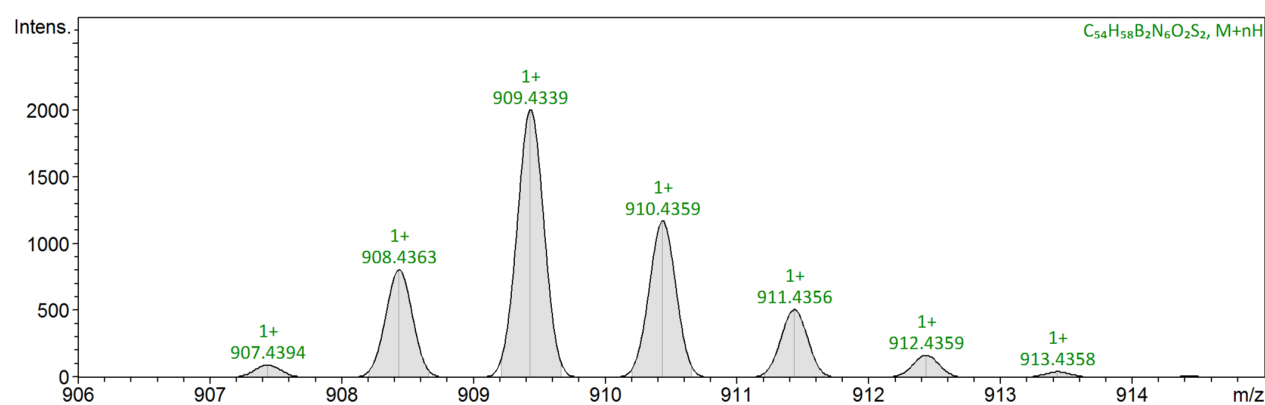
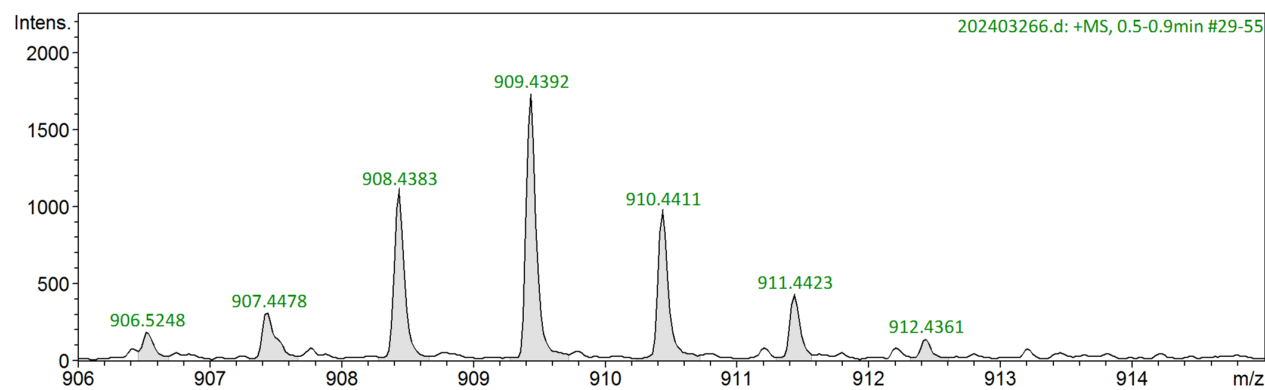
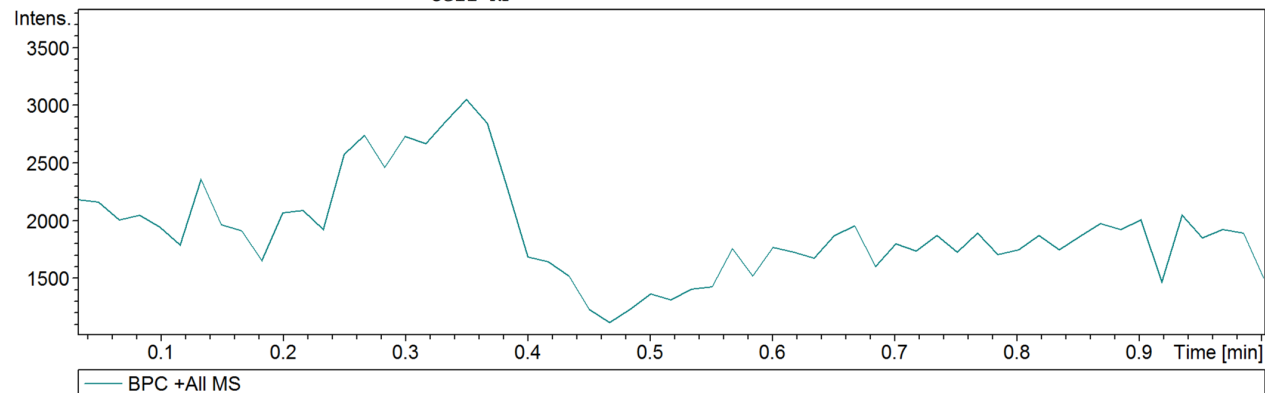


Fig. S1. HR-ESI-MS spectrum of 4-anti (middle) and the isotope pattern (bottom).

Acquisition Parameter

Source Type	ESI	Ion Polarity	Positive	Set Nebulizer	0.3 Bar
Focus	Not active	Set Capillary	4500 V	Set Dry Heater	180 °C
Scan Begin	100 m/z	Set End Plate	-400 V	Set Dry Gas	4.0 l/min
Scan End	3000 m/z	Collision Cell RF	650.0 Vpp	Set Divert Valve	Source

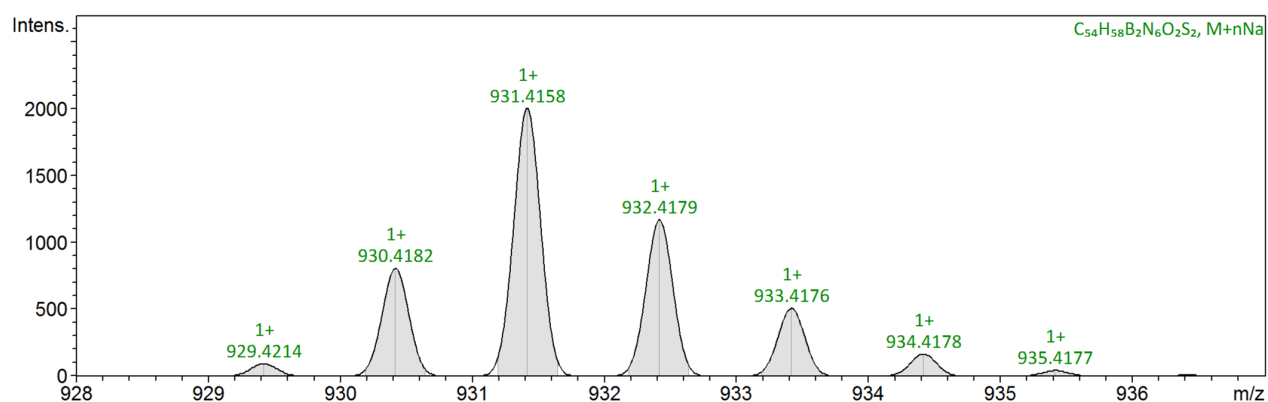
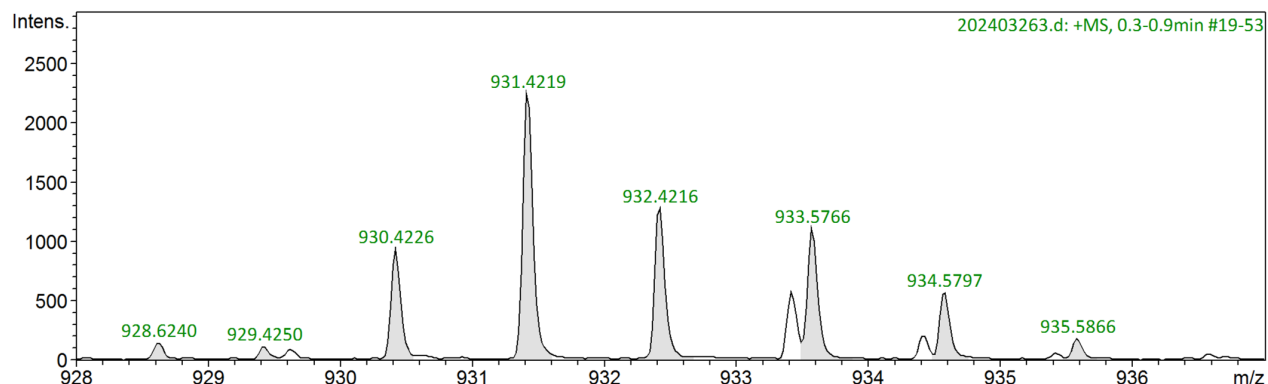
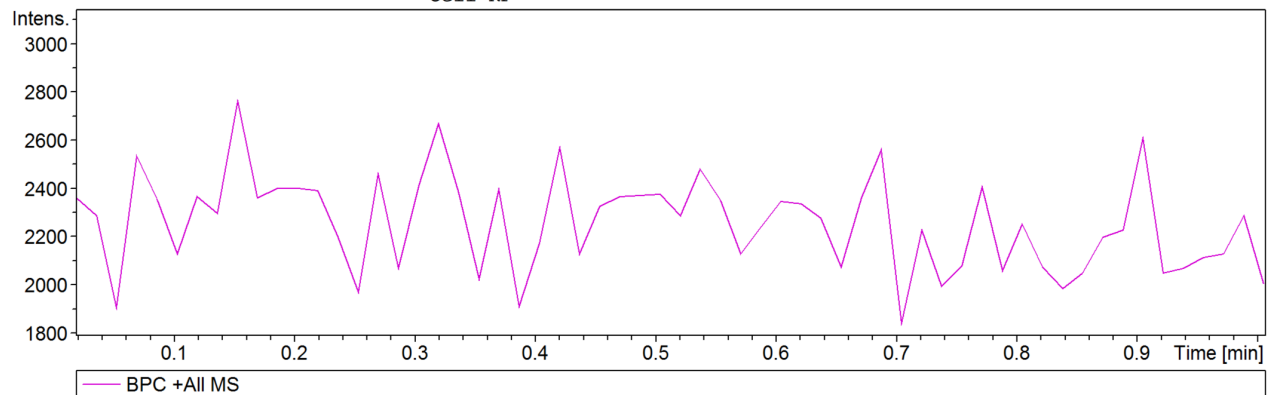


Fig. S2. HR-ESI-MS spectrum of 4-syn (middle) and the isotope pattern (bottom).

Acquisition Parameters

Source Type	ESI	Ion Polarity	Positive	Set Nebulizer	0.3 Bar
Focus	Not active	Set Capillary	4500 V	Set Dry Heater	180 °C
Scan Begin	100 m/z	Set End Plate	-400 V	Set Dry Gas	4.0 l/min
Scan End	3000 m/z	OffCollision Cell RF	650.0 Vpp	Set Divert Valve	Source

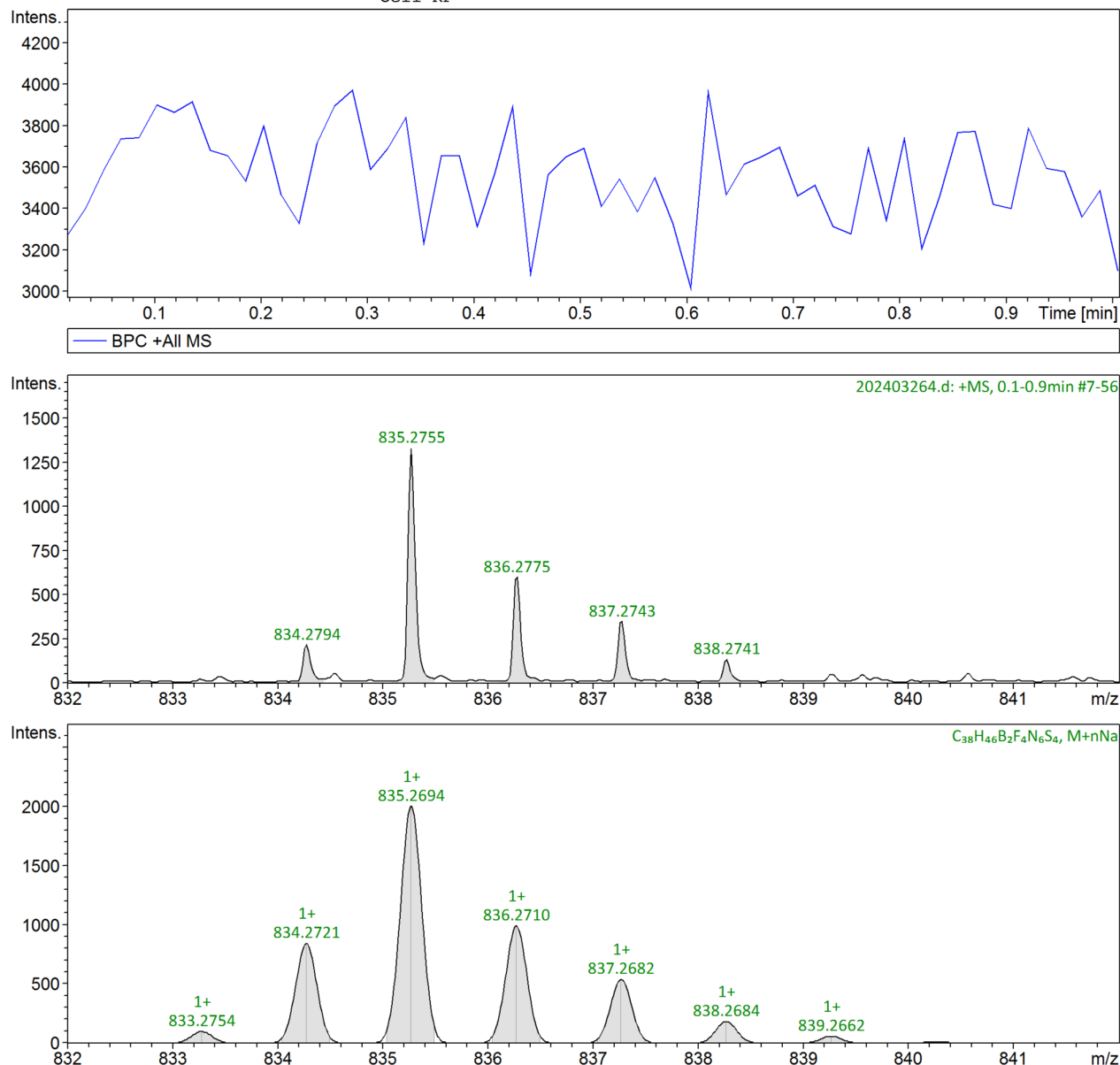


Fig. S3. HR-ESI-MS spectrum of **6** (middle) and the isotope pattern (bottom).

iii. NMR Spectra

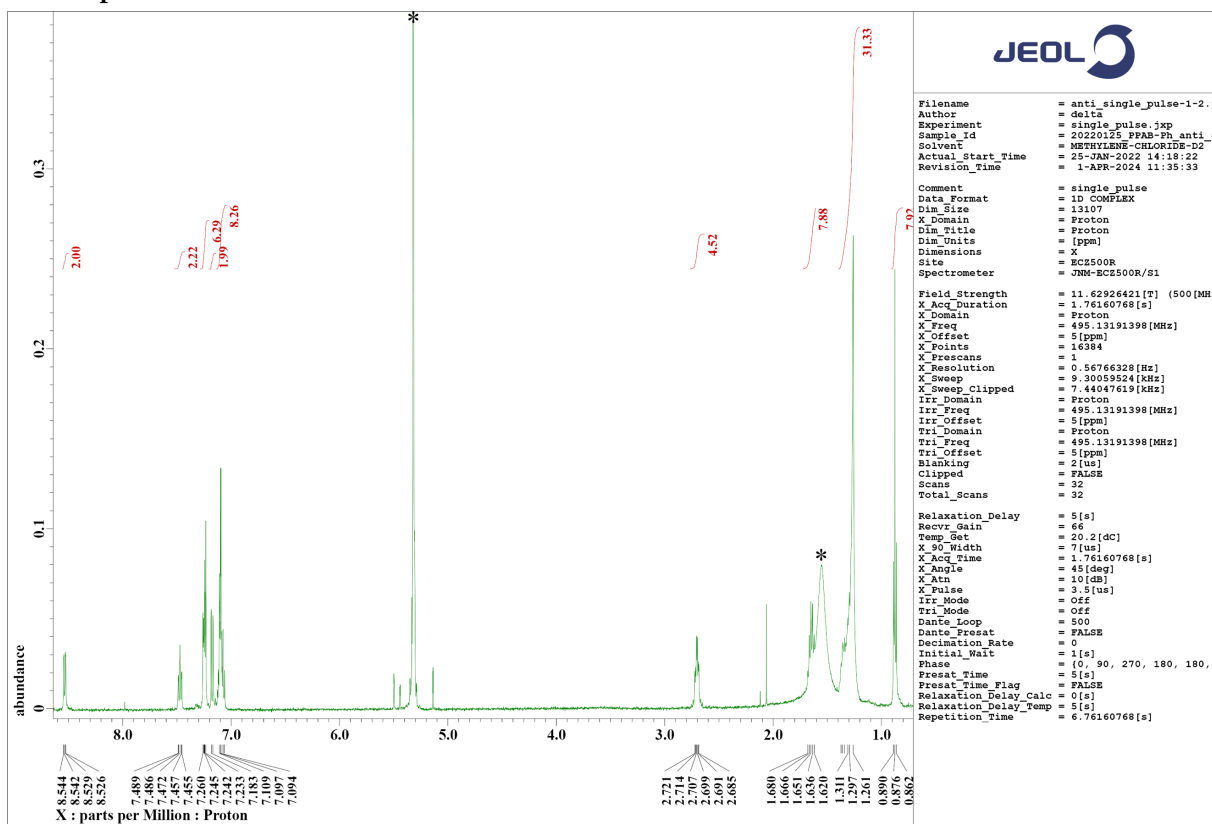


Fig. S4. ^1H NMR spectrum of **4-anti** in CD_2Cl_2 . * indicates a residual solvent signal.

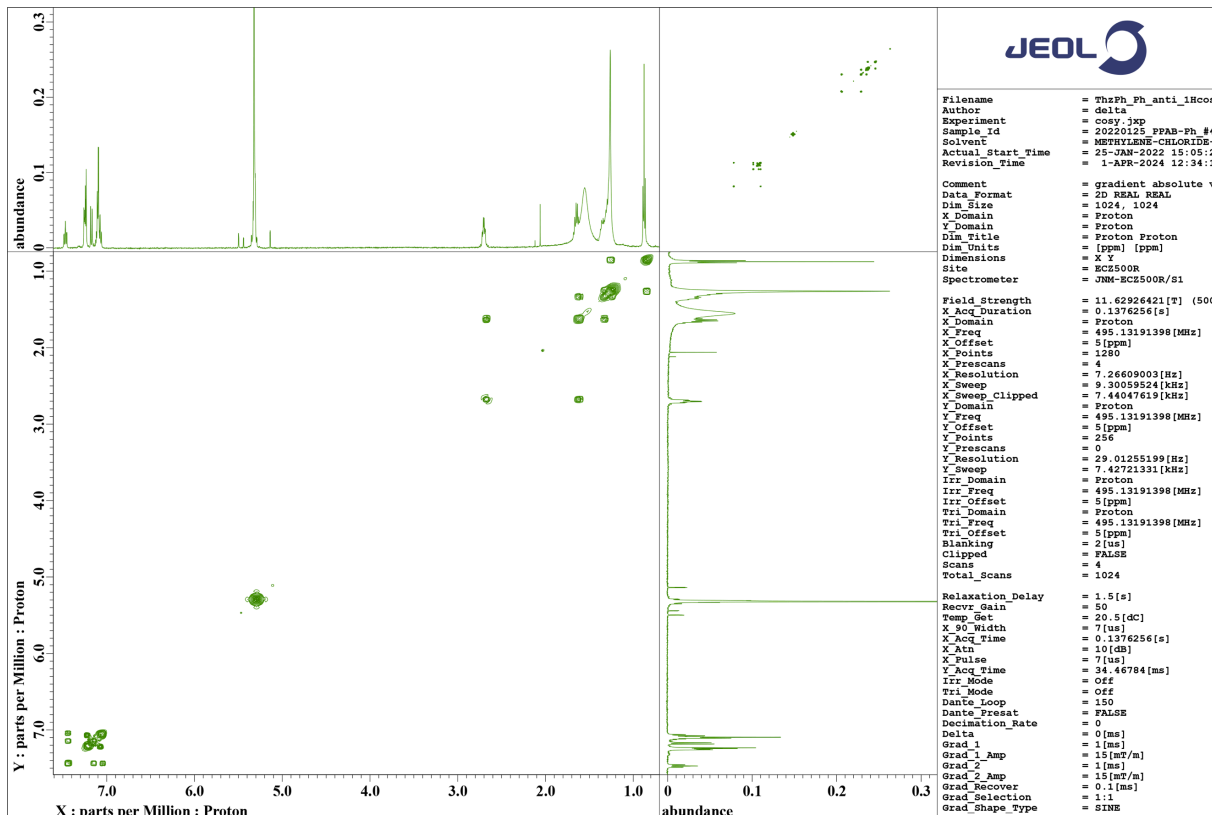


Fig. S5. ^1H - ^1H COSY spectrum of **4-anti** in CD_2Cl_2 .

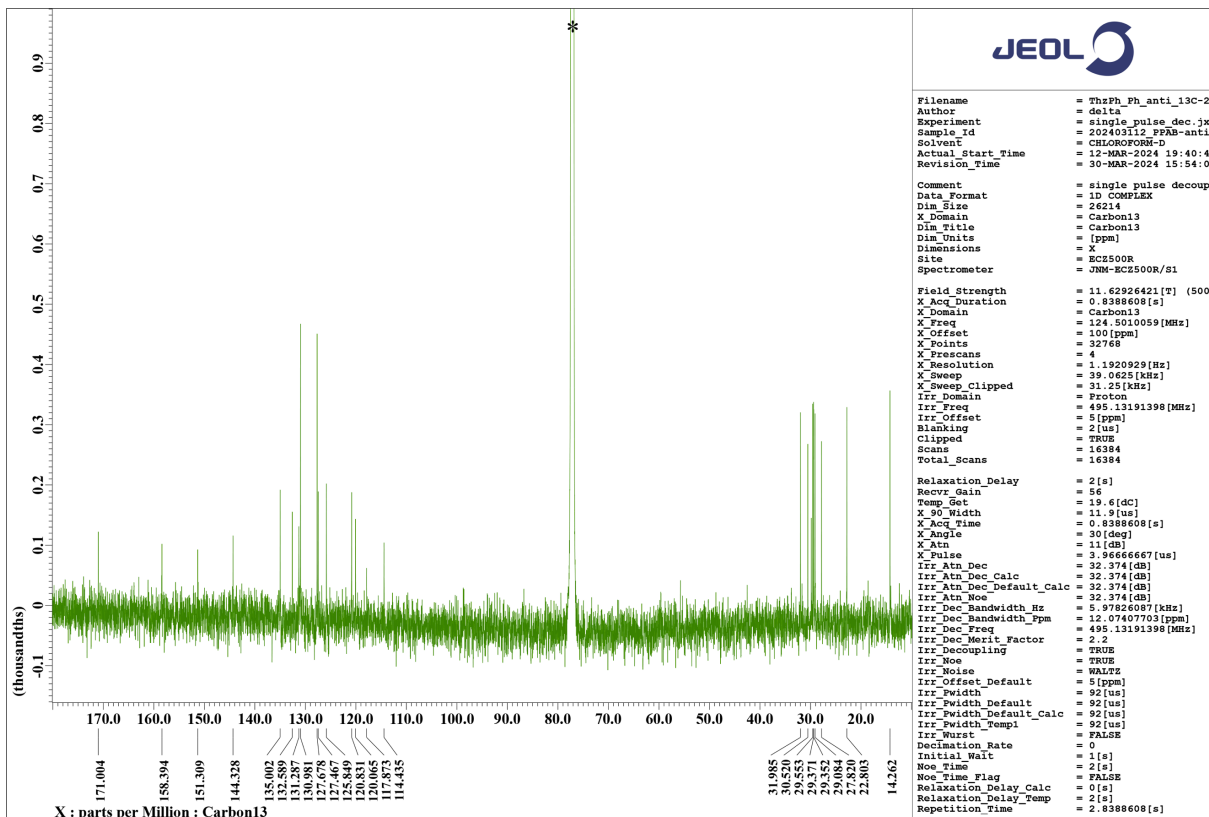


Fig. S6. ^{13}C NMR spectrum of 4-*anti* in CDCl_3 . * indicates a residual solvent signal.

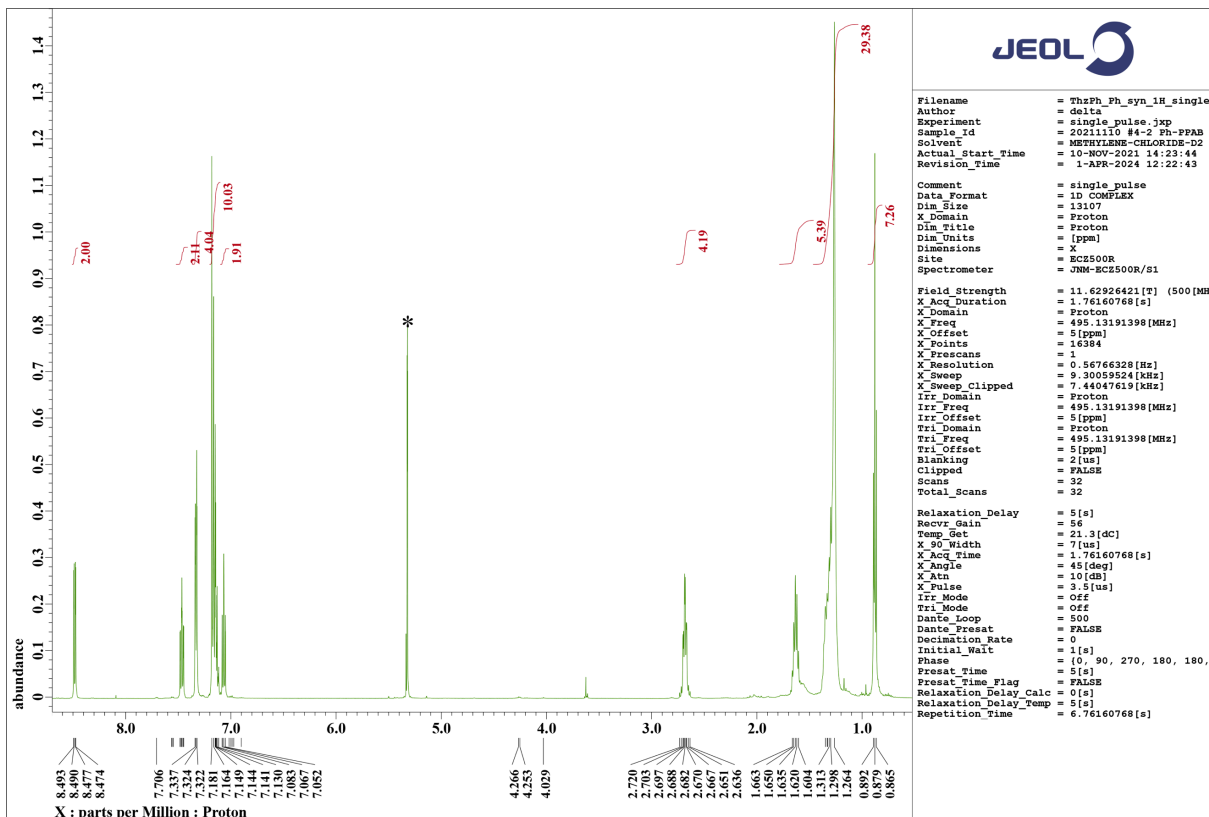


Fig. S7. ^1H NMR spectrum of 4-*syn* in CD_2Cl_2 . * indicates a residual solvent signal.

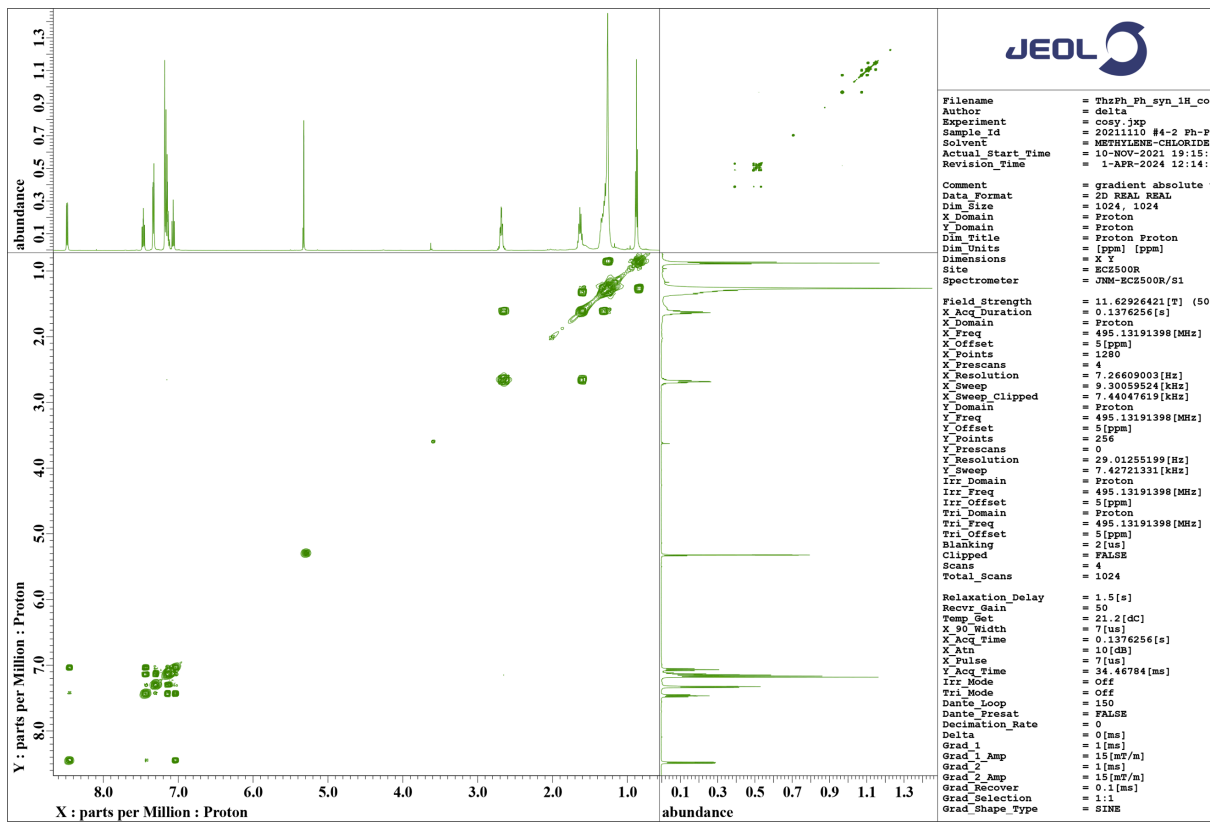


Fig. S8. ^1H - ^1H COSY spectrum of 4-syn in CD_2Cl_2 .

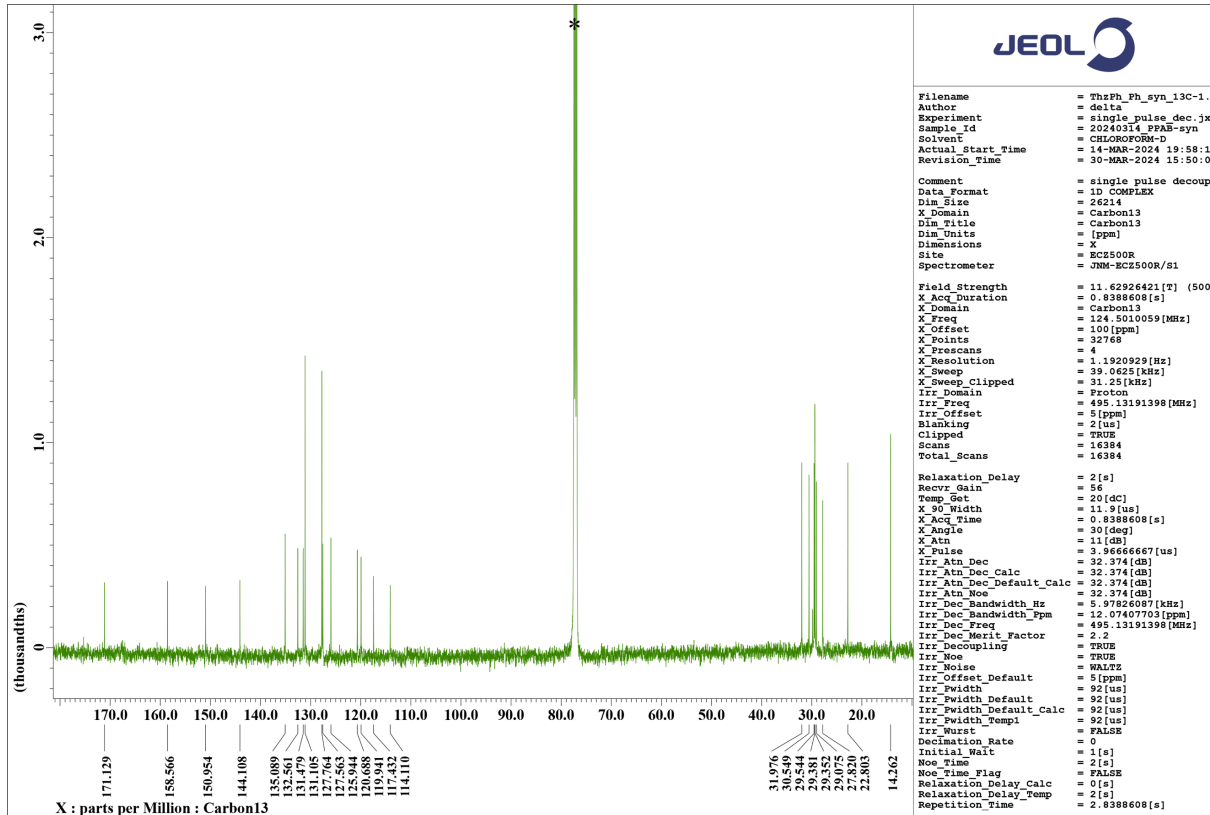


Fig. S9. ^{13}C NMR spectrum of 4-syn in CDCl_3 . * indicates a residual solvent signal.

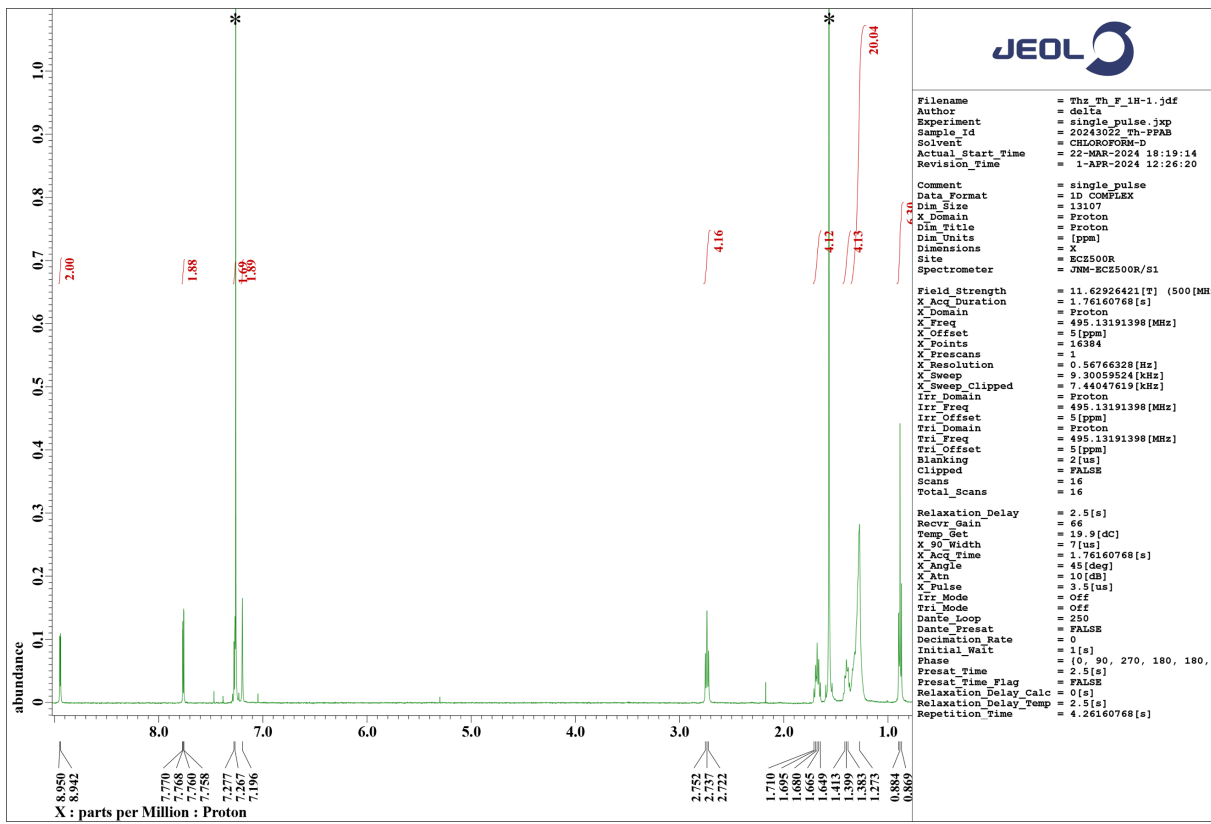


Fig. S10. ^1H NMR spectrum of 6 in CDCl_3 . * indicates a residual solvent signal.

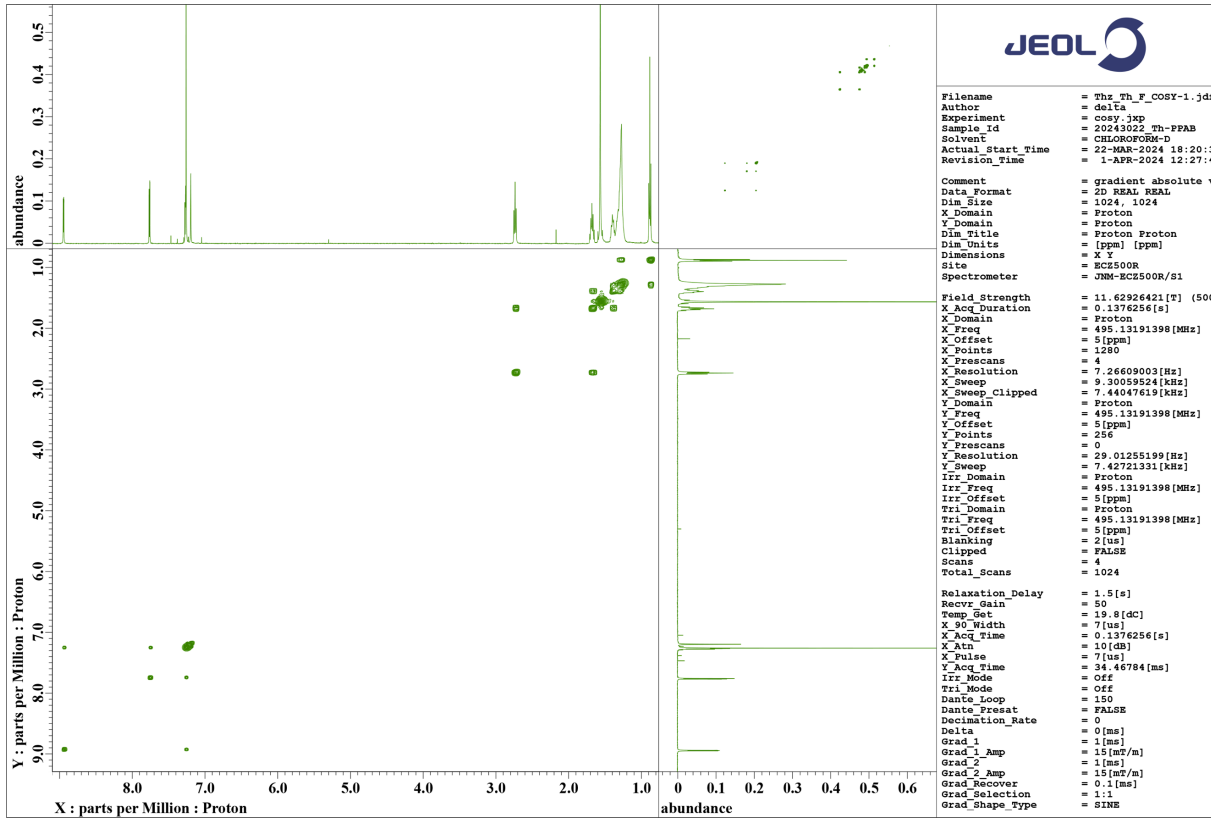


Fig. S11. ^1H - ^1H COSY spectrum of 6 in CDCl_3 .

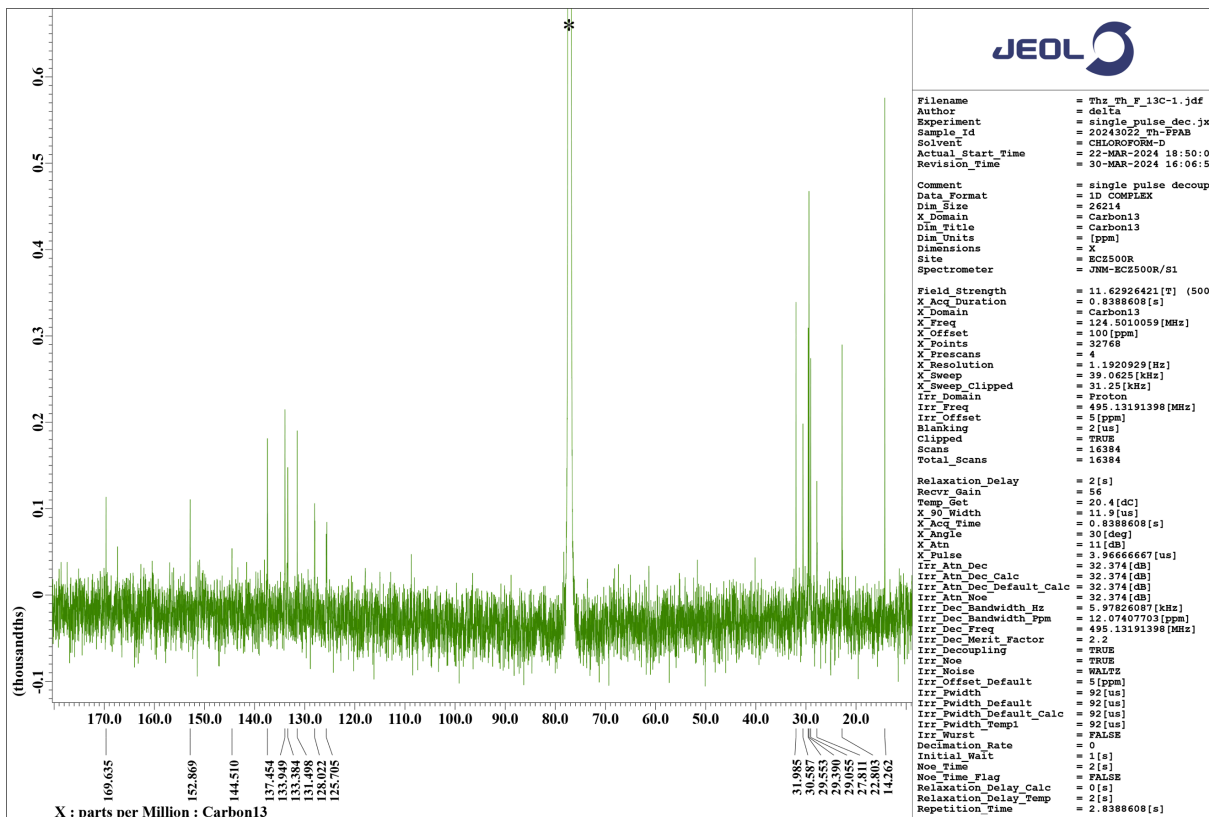


Fig. S12. ^{13}C NMR spectrum of **6** in CDCl_3 . * indicates a residual solvent signal.

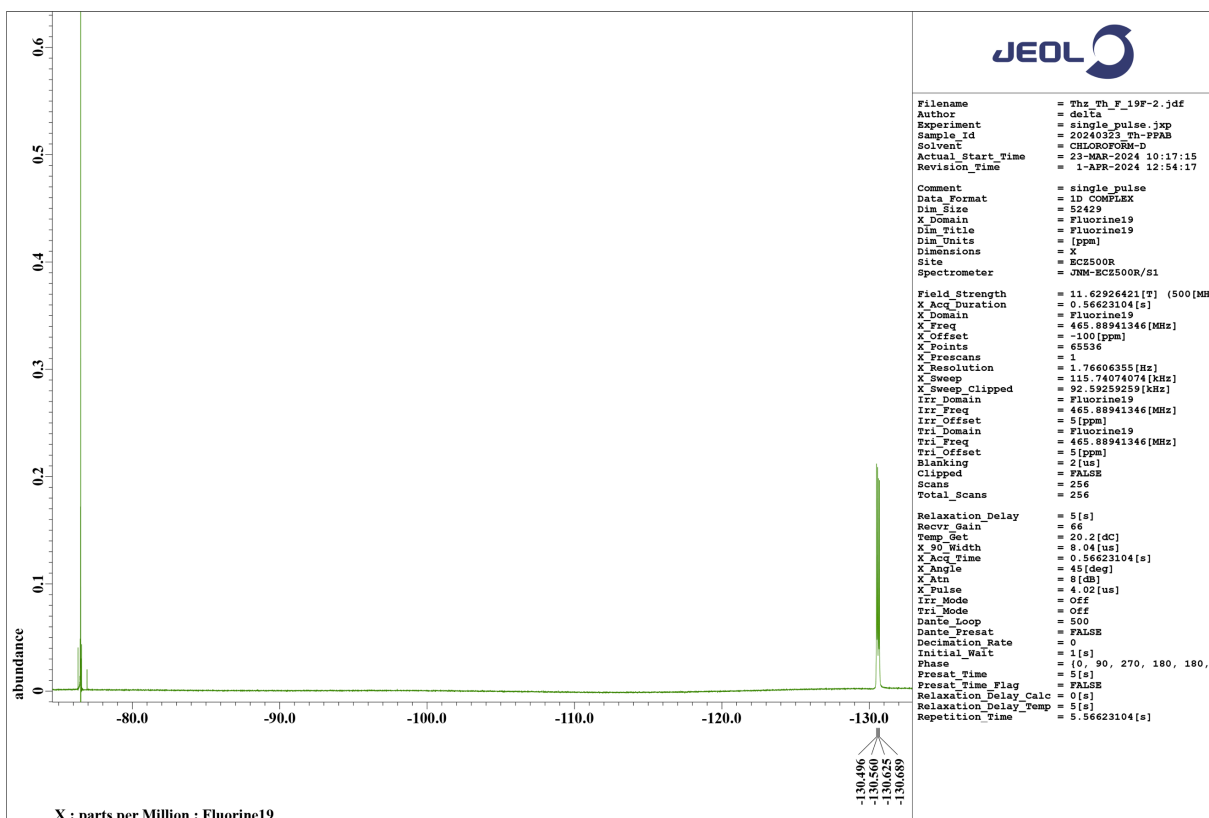


Fig. S13. ^{19}F NMR spectrum of **6** in CDCl_3 .

iv. Crystallographic Data

Table S1. Crystallographic data.

Compound	4-anti	6
Empirical formula	C ₅₄ H ₅₈ B ₂ N ₆ O ₂ S ₂	C ₃₈ H ₄₆ B ₂ F ₄ N ₆ S ₄
Formula weight	908.80	812.67
Temperature (K)	100	100
Wavelength (Å)	0.71073 (MoKα)	0.71073 (MoKα)
Crystal system	monoclinic	triclinic
Space group	P2 ₁ /c (no. 14)	$\bar{P}1$ (no. 2)
Unit cell dimensions		
<i>a</i> (Å)	20.7040(10)	7.7011(3)
<i>b</i> (Å)	6.2953(3)	11.6851(6)
<i>c</i> (Å)	18.9378(9)	11.8911(6)
α (°)	90	75.307(4)
β (°)	108.615(5)	71.596(4)
γ (°)	90	76.096(4)
Volume (Å ³)	2339.2(2)	967.05(9)
<i>Z</i>	2	1
Density (calcd.) (g/cm ³)	1.290	1.395
μ (mm ⁻¹)	0.164	0.303
<i>F</i> (000)	964	426
Crystal size (mm ³)	0.26 × 0.10 × 0.01	0.22 × 0.05 × 0.01
θ (°) for data collection	2.076 to 30.797	1.830 to 27.989
Index ranges	$-29 \leq h \leq 28$ $-8 \leq k \leq 9$ $-25 \leq l \leq 27$	$-10 \leq h \leq 10$ $-15 \leq k \leq 15$ $-15 \leq l \leq 15$
Reflection collected	47021	18553
Unique reflections	6930 ($R_{\text{int}} = 0.0645$)	4659 ($R_{\text{int}} = 0.0560$)
Completeness	0.949	0.998
Absorption correction	multi-scan	multi-scan
Max. and min. transmission	0.723, 1.000	0.663, 1.000
Data/restrains/parameters	6930/93/382	4659/109/290
Goodness-of-fit on F^2	1.024	1.038
Final <i>R</i> indices [$I > 2\sigma(I)$]	0.0715	0.0476
<i>wR</i> 2 indices (all data)	0.1744	0.1065
Large diff. peak and hole	0.39, -0.46	0.32, -0.35
CCDC number	2342651	2343541

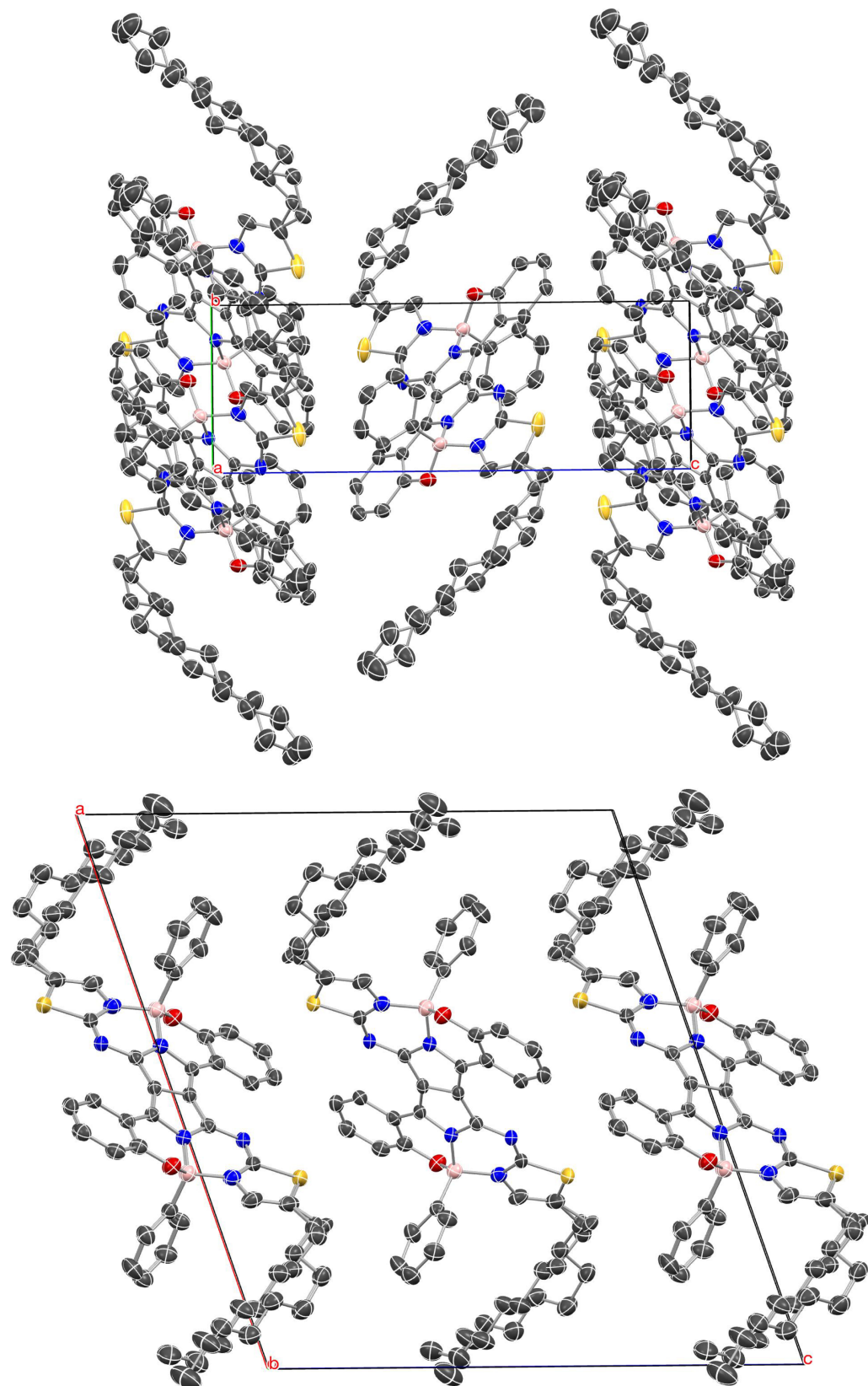


Fig. S14. Packing diagram of **4-anti**. The thermal ellipsoids are scaled to the 50% probability. Hydrogen atoms are omitted for clarity.

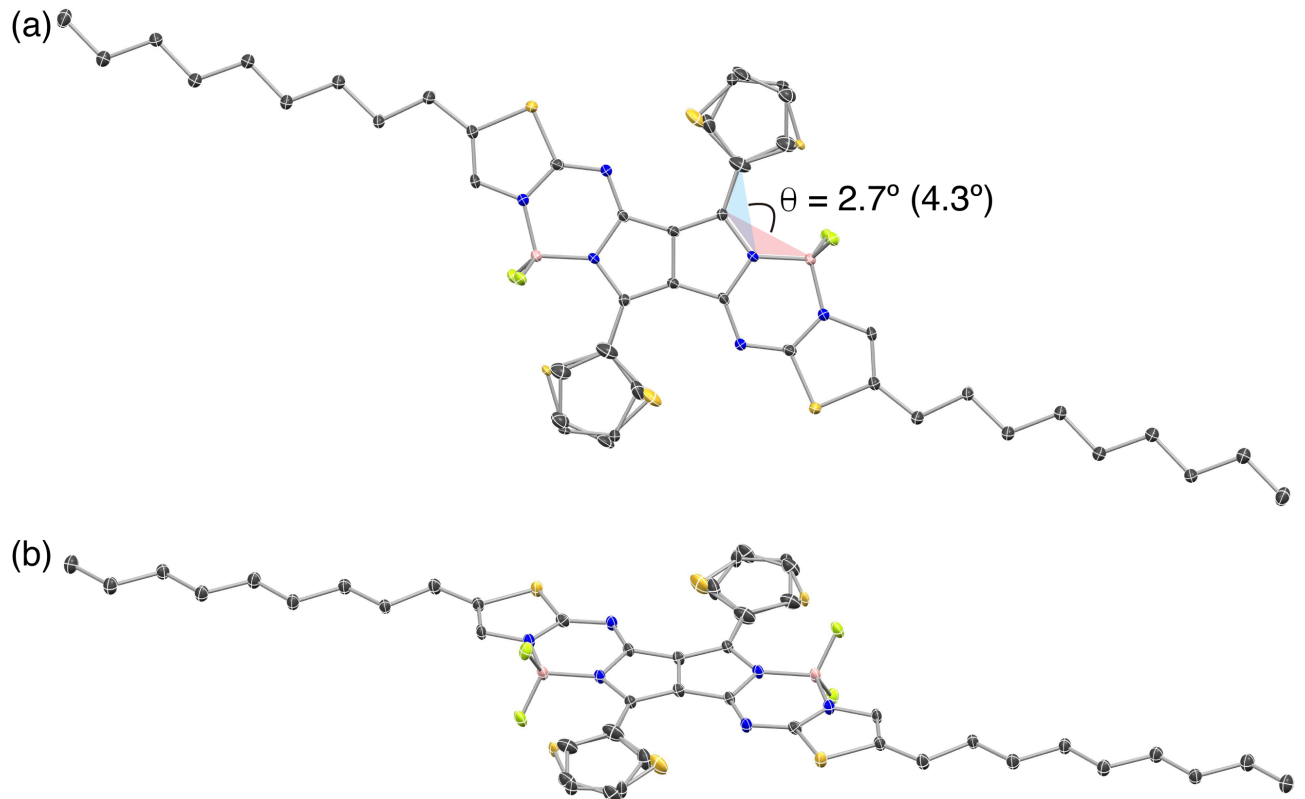


Fig. S15. X-Ray single-crystal structure of **6**, (a) top and (b) side views. The thermal ellipsoids are scaled to the 50% probability. Hydrogen atoms are omitted for clarity. The dihedral angle of the thienyl substituents with minor occupancy is shown in the parenthesis.

v. UV/vis Absorption, Excitation and Fluorescence Spectra

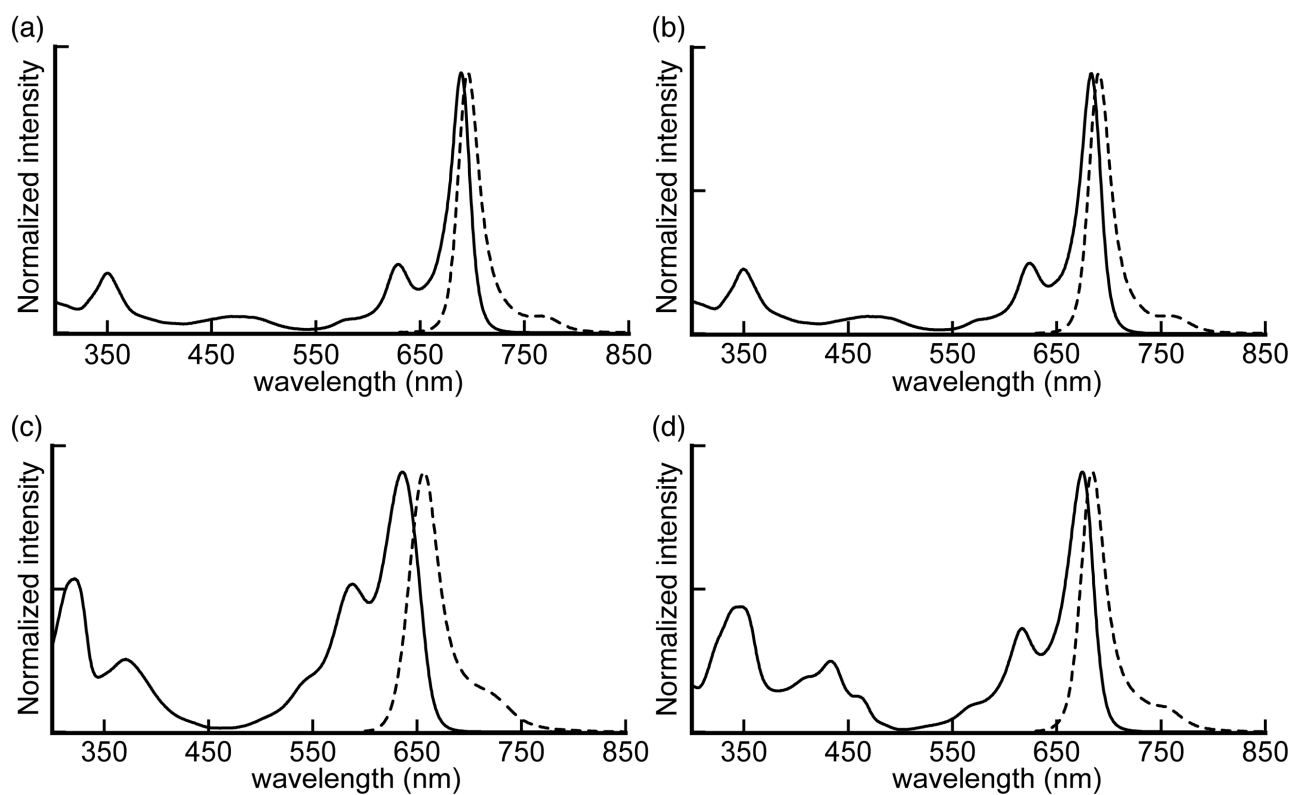


Fig. S16. Excitation (solid line) and fluorescence (dashed line) spectra of (a) **4-anti**, (b) **4-syn**, (c) **5** and (d) **6** in dichloromethane. The fluorescence spectra were measured by excitation at 550 nm for **5** and 600 nm for **4-anti**, **4-syn** and **6**. The excitation spectra were measured by monitoring the fluorescence intensities at 697 nm for **4-anti**, 691 nm for **4-syn**, 657 nm for **5** and 685 nm for **6**.

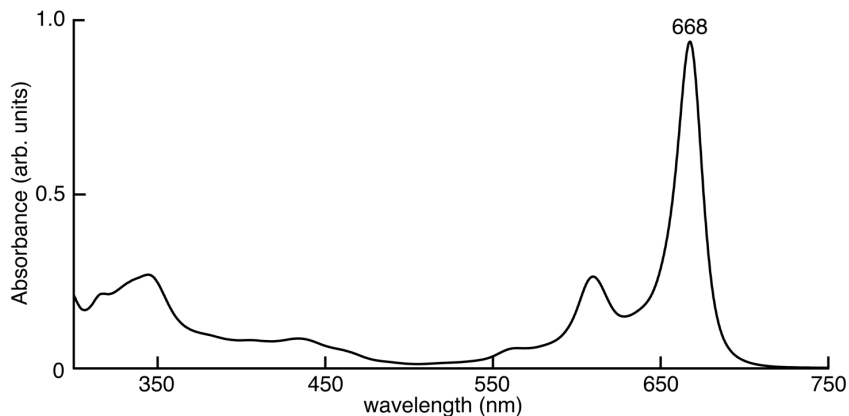


Fig. S17. UV/vis absorption spectrum of **3** in dichloromethane.

vi. Electrochemistry

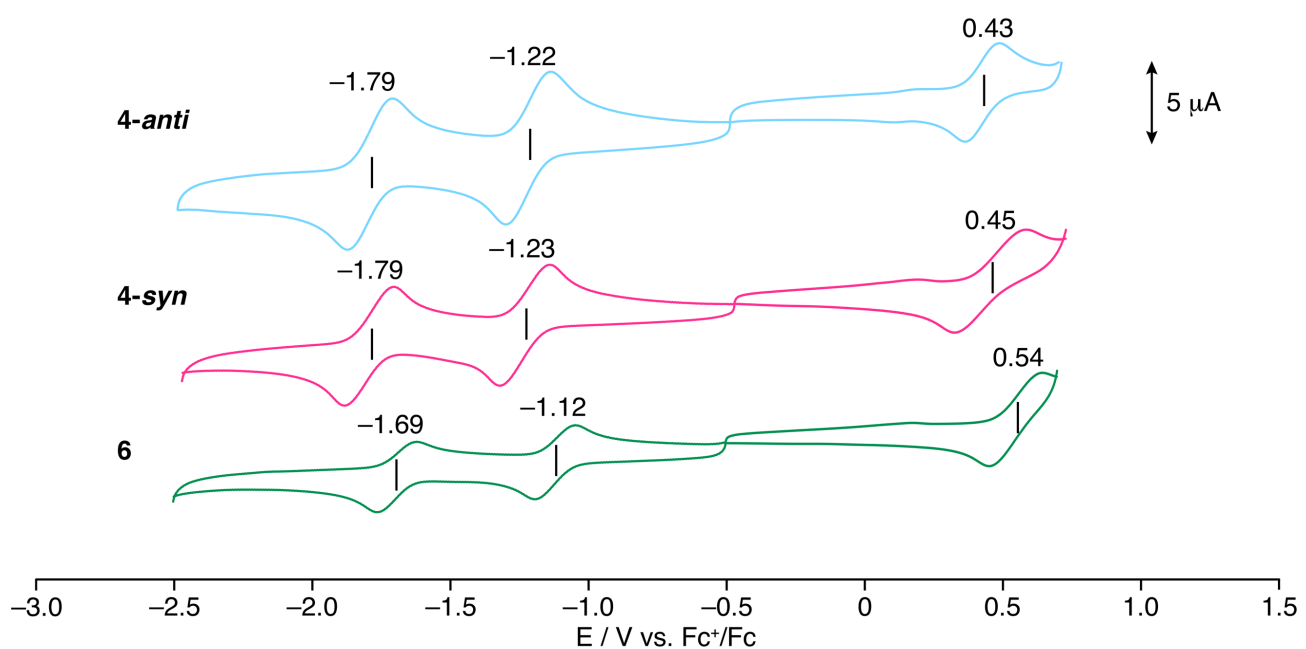


Fig. S18. Cyclic voltammograms of **4-anti**, **4-syn** and **6** (0.5 mM) in *o*-DCB containing 0.1 M TBAP at scan rate of 100 mV s⁻¹.

Table S2. Summary of electrochemical properties of **4-anti**, **4-syn**, **5** and **6**.

Compound	$E_{ox}^{1/2}$ [V]	$E_{red1}^{1/2}$ [V]	$E_{red2}^{1/2}$ [V]	$\Delta E^{[a]}$ [V]
4-anti	0.43	-1.22	-1.79	1.65
4-syn	0.45	-1.23	-1.79	1.68
5^[b]	0.69 ^[c]	-1.13		1.82
6	0.54	-1.12	-1.69	1.66

[a] $\Delta E = E_{ox}^{1/2} - E_{red1}^{1/2}$. [b] From ref. 10. [c] Potential was determined from the differential pulse voltammogram.

vii. DFT and TDDFT Calculations

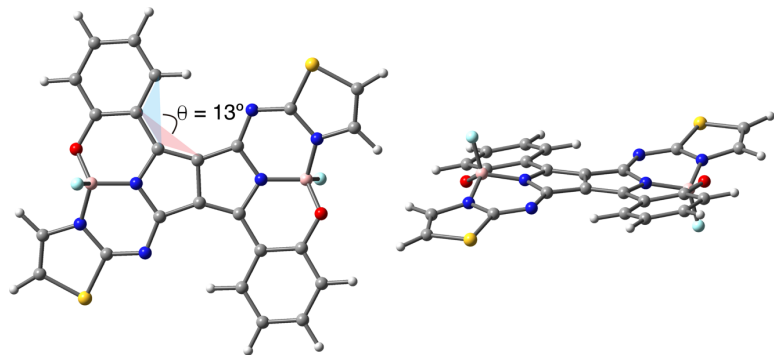


Fig. S19. Optimized structures of **3M-anti** (left: top view and right: side view) at the S_0 state at the ω B97XD/6-31G(d) level.

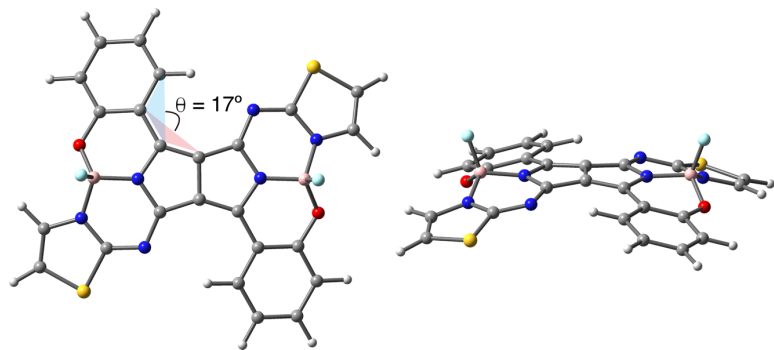


Fig. S20. Optimized structures of **3M-syn** (left: top view and right: side view) at the S_0 state at the ω B97XD/6-31G(d) level.

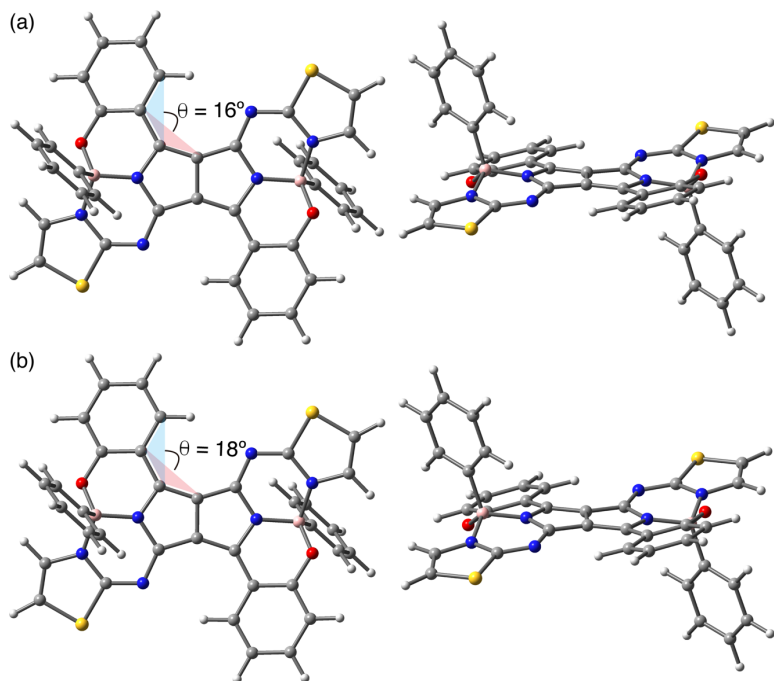


Fig. S21. Optimized structures of **4M-anti** (left: top view and right: side view) at the (a) S_0 and (b) S_1 states at the ω B97XD/6-31G(d) level.

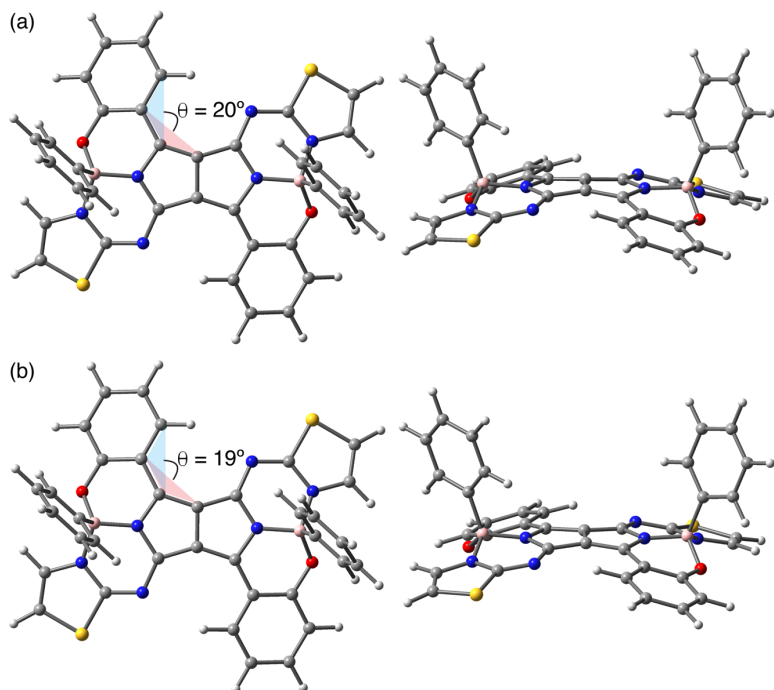


Fig. S22. Optimized structures of **4M-syn** (left: top view and right: side view) at the (a) S_0 and (b) S_1 states at the ω B97XD/6-31G(d) level.

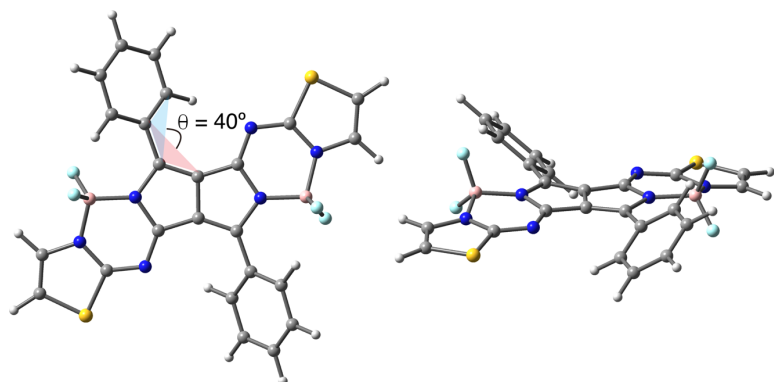


Fig. S23. Optimized structures of **5M** (left: top view and right: side view) at the S_0 state at the ω B97XD/6-31G(d) level.

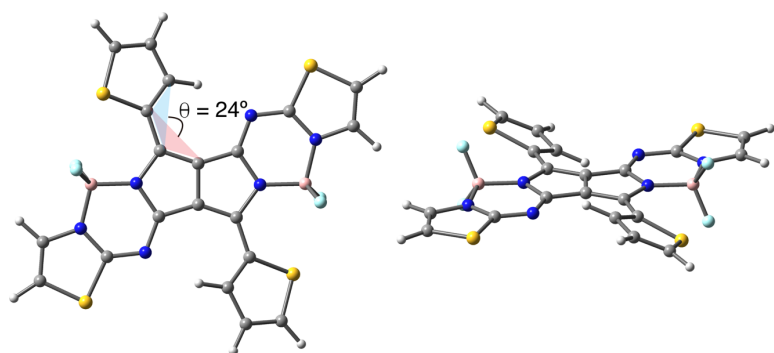


Fig. S24. Optimized structures of **6M** (left: top view and right: side view) at the S_0 state at the ω B97XD/6-31G(d) level.

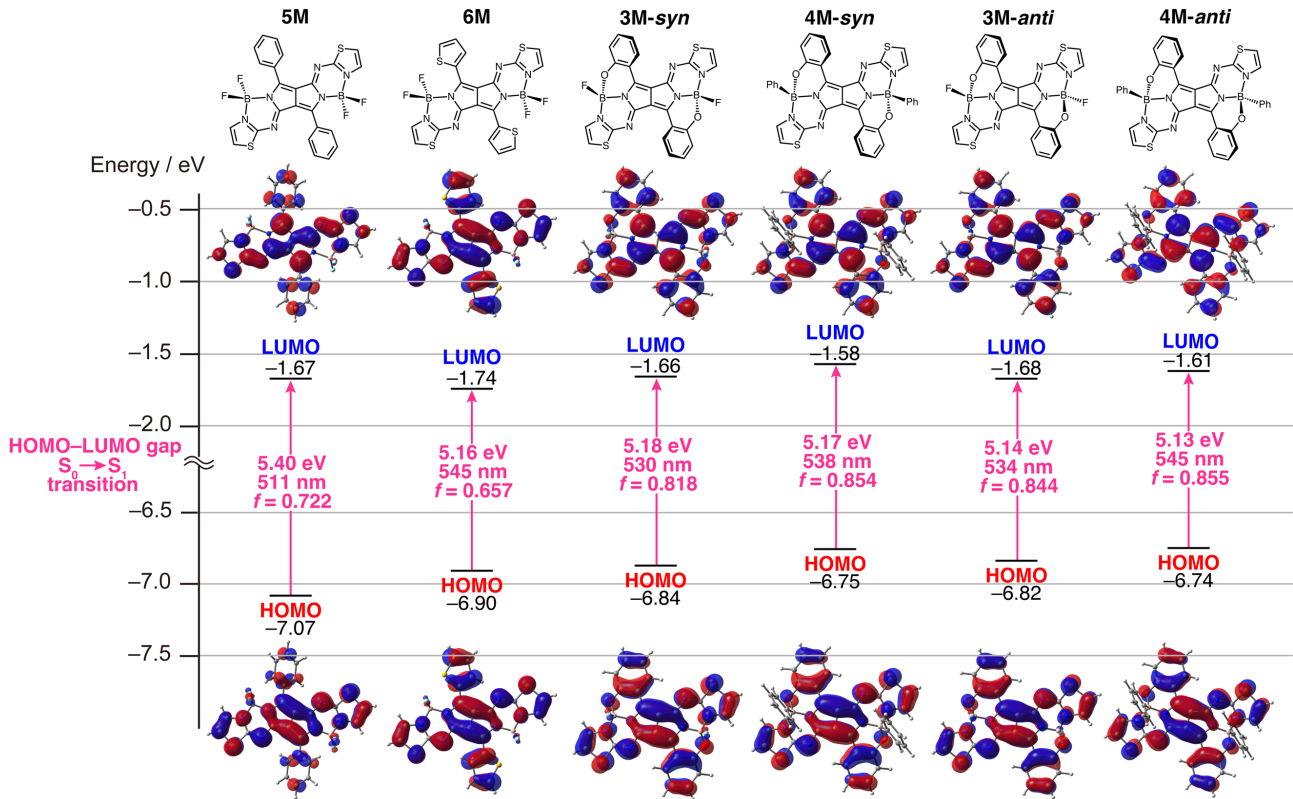


Fig. S25. Frontier molecular orbital diagrams of 3M-anti, 3M-syn, 4M-anti, 4M-syn, 5M and 6M at the ω B97XD/6-31G(d) level of theory. HOMO-LUMO energy gaps and S_0 -to- S_1 transitions estimated by the TDDFT calculations at the ω B97XD/6-31G(d) level of theory are shown.

Table S3. Selected transition energies, oscillator strength and major contributions of **3M-anti** calculated by the TDDFT method (ω B97XD/6-31G(d)). The S_0 -to- S_1 transition is highlighted in bold.

	wavelength [nm]	f ^[a]	Major contributions (weight%) ^[b]
$S_0 \rightarrow S_1$	534	0.844	HOMO \rightarrow LUMO (98%)
$S_0 \rightarrow S_2$	404	0.000	H-5 \rightarrow LUMO (63%), H-1 \rightarrow LUMO (27%)
$S_0 \rightarrow S_3$	353	0.000	H-5 \rightarrow LUMO (31%), H-1 \rightarrow LUMO (51%), HOMO \rightarrow L+1 (11%)
$S_0 \rightarrow S_4$	352	0.227	H-2 \rightarrow LUMO (91%)
$S_0 \rightarrow S_5$	324	0.000	H-3 \rightarrow LUMO (32%), H-1 \rightarrow LUMO (13%), HOMO \rightarrow L+1 (47%)

[a] Oscillator strength. [b] H and L denote the HOMO and LUMO, respectively.

Table S4. Selected transition energies, oscillator strength and major contributions of **3M-syn** calculated by the TDDFT method (ω B97XD/6-31G(d)). The S_0 -to- S_1 transition is highlighted in bold.

	wavelength [nm]	f ^[a]	Major contributions (weight%) ^[b]
$S_0 \rightarrow S_1$	530	0.818	HOMO \rightarrow LUMO (98%)
$S_0 \rightarrow S_2$	397	0.000	H-5 \rightarrow LUMO (60%), H-1 \rightarrow LUMO (29%)
$S_0 \rightarrow S_3$	351	0.000	H-5 \rightarrow LUMO (34%), H-1 \rightarrow LUMO (48%), HOMO \rightarrow L+1 (11%)
$S_0 \rightarrow S_4$	350	0.222	H-2 \rightarrow LUMO (90%)
$S_0 \rightarrow S_5$	324	0.005	H-3 \rightarrow LUMO (30%), H-1 \rightarrow LUMO (14%), HOMO \rightarrow L+1 (48%)

[a] Oscillator strength. [b] H and L denote the HOMO and LUMO, respectively.

Table S5. Selected transition energies, oscillator strength and major contributions of **4M-anti** calculated by the TDDFT method (ω B97XD/6-31G(d)). The S_0 -to- S_1 transition is highlighted in bold.

	wavelength [nm]	f ^[a]	Major contributions (weight%) ^[b]
$S_0 \rightarrow S_1$	545	0.855	HOMO →LUMO (97%)
$S_0 \rightarrow S_2$	419	0.000	H-9→LUMO (69%), H-3→LUMO (25%)
$S_0 \rightarrow S_3$	388	0.000	H-1→LUMO (84%)
$S_0 \rightarrow S_4$	387	0.176	H-2→LUMO (92%)
$S_0 \rightarrow S_5$	328	0.000	H-7→LUMO (25%), HOMO→L+1 (56%)

[a] Oscillator strength. [b] H and L denote the HOMO and LUMO, respectively.

Table S6. Selected transition energies, oscillator strength and major contributions of **4M-syn** calculated by the TDDFT method (ω B97XD/6-31G(d)). The S_0 -to- S_1 transition is highlighted in bold.

	wavelength [nm]	f ^[a]	Major contributions (weight%) ^[b]
$S_0 \rightarrow S_1$	538	0.854	HOMO →LUMO (97%)
$S_0 \rightarrow S_2$	411	0.000	H-9→LUMO (65%), H-3→LUMO (28%)
$S_0 \rightarrow S_3$	386	0.000	H-1→LUMO (83%)
$S_0 \rightarrow S_4$	384	0.172	H-2→LUMO (92%)
$S_0 \rightarrow S_5$	327	0.004	H-7→LUMO (23%), HOMO→L+1 (57%)

[a] Oscillator strength. [b] H and L denote the HOMO and LUMO, respectively.

Table S7. Selected transition energies, oscillator strength and major contributions of **5M** calculated by the TDDFT method (ω B97XD/6-31G(d)). The S_0 -to- S_1 transition is highlighted in bold.

	wavelength [nm]	f ^[a]	Major contributions (weight%) ^[b]
$S_0 \rightarrow S_1$	511	0.722	HOMO →LUMO (97%)
$S_0 \rightarrow S_2$	386	0.000	H-6→LUMO (16%), H-5→LUMO (69%), H-1→LUMO (10%)
$S_0 \rightarrow S_3$	333	0.005	H-1→LUMO (60%), HOMO→L+1 (20%)
$S_0 \rightarrow S_4$	315	0.691	H-2→LUMO (92%)
$S_0 \rightarrow S_5$	299	0.012	H-3→LUMO (86%)

[a] Oscillator strength. [b] H and L denote the HOMO and LUMO, respectively.

Table S8. Selected transition energies, oscillator strength and major contributions of **6M** calculated by the TDDFT method (ω B97XD/6-31G(d)). The S_0 -to- S_1 transition is highlighted in bold.

	wavelength [nm]	f ^[a]	Major contributions (weight%) ^[b]
$S_0 \rightarrow S_1$	545	0.657	HOMO →LUMO (98%)
$S_0 \rightarrow S_2$	389	0.000	H-6→LUMO (16%), H-5→LUMO (50%), H-1→LUMO (22%)
$S_0 \rightarrow S_3$	346	0.000	H-6→LUMO (13%), H-5→LUMO (14%), H-1→LUMO (42%), HOMO→L+1 (26%)
$S_0 \rightarrow S_4$	344	0.710	H-2→LUMO (93%)
$S_0 \rightarrow S_5$	308	0.000	H-1→LUMO (29%), HOMO→L+1 (59%)

[a] Oscillator strength. [b] H and L denote the HOMO and LUMO, respectively.

viii. Estimation of Dissymmetry Factors of Theoretical CD and CPL

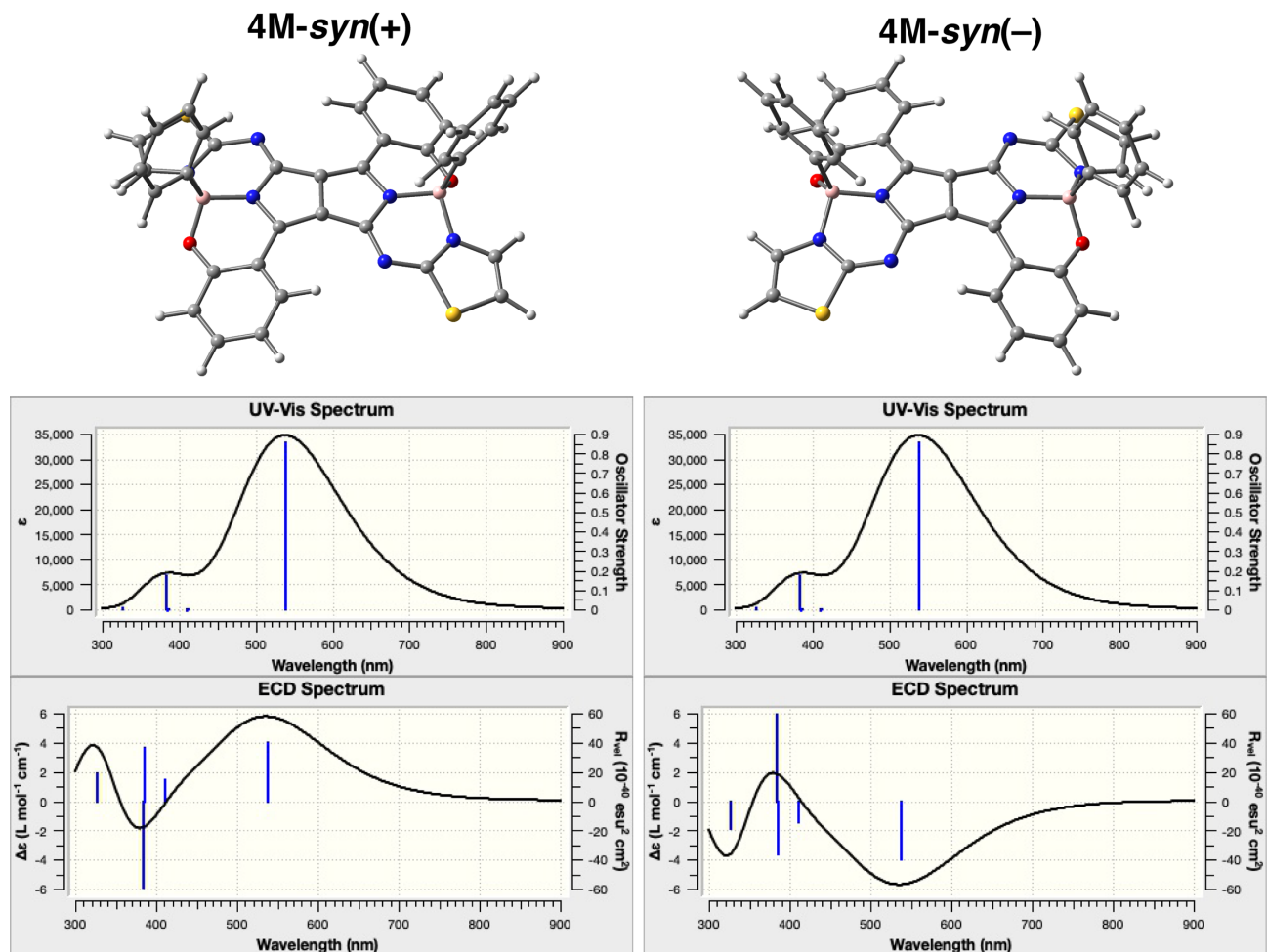
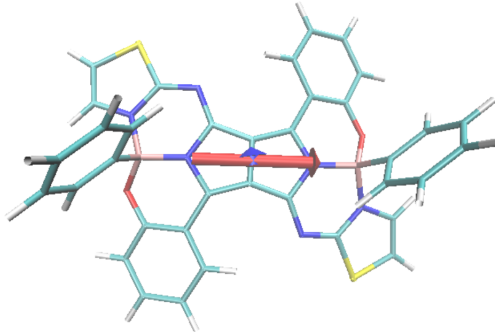


Fig. S26. Theoretical UV/vis absorption (top) and CD (bottom) spectra of *4M-syn(+)* (left) and *4M-syn(-)* (right) at the ω B97XD/6-31G(d) level of theory.

Transition electric (TEDM) and transition magnetic (TMDM) dipole moments were generated from the TDDFT data by Multiwfn¹¹ and visualized by VMD.¹²

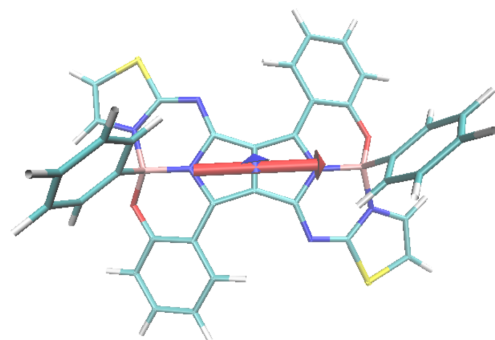
Table S9. S₀-to-S₁ transition properties of **4M-syn(+)** calculated by the TDDFT method (ω B97XD/6-31G(d)). In the structure of **4M-syn(+)** at the S₀ state, the spatial arrangement of the transition electric and magnetic dipole moment vectors for the S₀-to-S₁ transition is shown.



	$\lambda^{[a]}$ [nm]	$\mu^{[b]}$ [10^{-18} esu·cm]	$m^{[c]}$ [10^{-21} erg·G ⁻¹]	$\theta_{\mu \cdot m}^{[d]}$ [°]	$R^{[e]}$ [10^{-39} esu·erg·cm·G ⁻¹]	g_{CD}
S ₀ -to-S ₁	538	9.89	2.71	80.8	4.29	1.75×10^{-4}

[a] Wavelength. [b] TEDM. [c] TMDM. [d] Angle of TEDM and TMDM. [e] Rotatory strength defined as $R = |\mu| \cdot |m| \cdot \cos \theta_{\mu \cdot m}$.

Table S10. S₁-to-S₀ detransition properties of **4M-syn(+)** calculated by the TDDFT method (ω B97XD/6-31G(d)). In the structure of **4M-syn(+)** at the S₁ state, the spatial arrangement of the transition electric and magnetic dipole moment vectors for the S₁-to-S₀ detransition is shown.



	$\lambda^{[a]}$ [nm]	$\mu^{[b]}$ [10^{-18} esu·cm]	$m^{[c]}$ [10^{-21} erg·G ⁻¹]	$\theta_{\mu \cdot m}^{[d]}$ [°]	$R^{[e]}$ [10^{-39} esu·erg·cm·G ⁻¹]	g_{CPL}
S ₁ -to-S ₀	567	10.1	3.08	84.1	3.22	1.26×10^{-4}

[a] Wavelength. [b] TEDM. [c] TMDM. [d] Angle of TEDM and TMDM. [e] Rotatory strength defined as $R = |\mu| \cdot |m| \cdot \cos \theta_{\mu \cdot m}$.

ix. References

1. T. Harada, H. Hayakawa, M. Watanabe, M. Takamoto, *Rev. Sci. Instrum.*, 2016, **87**, 075102.
2. JASCO Co. Ltd., CPL technical note, Ishikawa, Hachioji, Tokyo, 2006.
3. G. Sheldrick, *Acta Crystallogr. Sect. A*, 2015, **71**, 3–8.
4. G. Sheldrick, *Acta Crystallographica Section C*, 2015, **71**, 3–8.
5. M. J. Frisch, G. W. Trucks, H. B. Schlegel, G. E. Scuseria, M. A. Robb, J. R. Cheeseman, G. Scalmani, V. Barone, G. A. Petersson, H. Nakatsuji, X. Li, M. Caricato, A. V. Marenich, J. Bloino, B. G. Janesko, R. Gomperts, B. Mennucci, H. P. Hratchian, J. V. Ortiz, A. F. Izmaylov, J. L. Sonnenberg, D. Williams-Young, F. Ding, F. Lipparini, F. Egidi, J. Goings, B. Peng, A. Petrone, T. Henderson, D. Ranasinghe, V. G. Zakrzewski, J. Gao, N. Rega, G. Zheng, W. Liang, M. Hada, M. Ehara, K. Toyota, R. Fukuda, J. Hasegawa, M. Ishida, T. Nakajima, Y. Honda, O. Kitao, H. Nakai, T. Vreven, K. Throssell, J. A. Montgomery, Jr., J. E. Peralta, F. Ogliaro, M. J. Bearpark, J. J. Heyd, E. N. Brothers, K. N. Kudin, V. N. Staroverov, T. A. Keith, R. Kobayashi, J. Normand, K. Raghavachari, A. P. Rendell, J. C. Burant, S. S. Iyengar, J. Tomasi, M. Cossi, J. M. Millam, M. Klene, C. Adamo, R. Cammi, J. W. Ochterski, R. L. Martin, K. Morokuma, O. Farkas, J. B. Foresman and D. J. Fox, *Gaussian 16 Rev. C.01*, (2019), Wallingford, CT.
6. J. D. Chai and M. Head-Gordon, *Phys. Chem. Chem. Phys.* 2008, **10**, 6615–6620.
7. B. P. Pritchard, D. Altarawy, B. Didier, T. D. Gibson and T. L. Windus, *J. Chem. Inf. Model.*, 2019, **59**, 4814–4820.
8. H. Langhals, T. Potrawa, H. Nöth and G. Linti, *Angew. Chem. Int. Ed. Engl.*, 1989, **28**, 478–480.
9. Z. Xiao, J. Subbiah, K. Sun, S. Ji, D. J. Jones, A. B. Holmes and W. W. H. Wong, *J. Mater. Chem. C* 2014, **2**, 1306–1313.
10. Y. Kage, S. Kang, S. Mori, M. Mamada, C. Adachi, D. Kim, H. Furuta and S. Shimizu, *Chem. Eur. J.* 2021, **27**, 5259–5267.
11. T. Lu and F. Chen, *J. Comput. Chem.* 2012, **33**, 580–592.
12. W. Humphrey, A. Dalke and K. Schulten, *J. Molec. Graphics* 1996, **14**, 33–38.

x. Appendix

Table Appx-1. Cartesian coordinates of the DFT optimized geometry of **3M-anti** at the ground state calculated at the level of ω B97XD/6-31G(d).

Imaginary Freq: 0

Total Energy (Hartree): -2446.3001

Symbol	X	Y	Z	Symbol	X	Y	Z		
1	S	-4.626	-3.166	-0.391	26	O	-3.925	1.819	-0.113
2	F	3.742	-0.692	-1.93	27	N	2.24	2.031	-0.046
3	N	-2.24	-2.031	0.046	28	N	-2.068	0.322	0.228
4	N	2.068	-0.322	-0.228	29	H	4.241	0.677	-0.03
5	N	-4.241	-0.677	0.03	30	H	-3.092	6.204	-0.565
6	H	3.092	-6.204	0.565	31	C	1.506	0.925	-0.125
7	C	-1.506	-0.925	0.125	32	C	-1.647	2.664	0.006
8	C	1.647	-2.664	-0.006	33	C	-0.79	3.776	-0.055
9	C	0.79	-3.776	0.055	34	H	0.281	3.615	0.045
10	H	-0.281	-3.615	-0.045	35	C	-1.137	1.323	0.103
11	C	1.137	-1.323	-0.103	36	C	0.105	0.713	-0.011
12	C	-0.105	-0.713	0.01	37	C	-1.303	5.043	-0.251
13	C	1.303	-5.043	0.251	38	H	-0.64	5.901	-0.293
14	H	0.64	-5.901	0.293	39	C	-2.685	5.21	-0.405
15	C	2.685	-5.21	0.405	40	C	3.558	1.838	0.055
16	C	-3.558	-1.838	-0.055	41	C	-3.051	2.839	-0.139
17	C	3.051	-2.839	0.139	42	C	-3.547	4.127	-0.355
18	O	3.925	-1.819	0.113	43	H	-4.619	4.251	-0.471
19	C	3.547	-4.127	0.355	44	C	5.6	0.821	0.165
20	H	4.619	-4.251	0.471	45	H	6.224	-0.06	0.109
21	C	-5.6	-0.821	-0.165	46	C	5.991	2.087	0.408
22	H	-6.224	0.06	-0.109	47	B	-3.521	0.602	0.563
23	C	-5.991	-2.087	-0.408	48	H	6.992	2.447	0.59
24	B	3.521	-0.602	-0.563	49	H	-6.992	-2.447	-0.59
25	S	4.626	3.166	0.391	50	F	-3.742	0.692	1.93

Table Appx-2. Cartesian coordinates of the DFT optimized geometry of **3M-syn** at the ground state calculated at the level of ω B97XD/6-31G(d).

Imaginary Freq: 0

Total Energy (Hartree): -2446.301

Symbol	X	Y	Z	Symbol	X	Y	Z
1 S	-4.538889	-3.136169	-0.572384	26 F	-3.998359	0.768223	1.804479
2 F	3.998362	-0.768221	1.804474	27 N	2.238753	2.011912	0.217662
3 N	-2.238752	-2.011912	0.217667	28 N	-2.075472	0.34231	0.402796
4 N	2.075472	-0.34231	0.402793	29 N	4.201503	0.646255	-0.118849
5 N	-4.201503	-0.646255	-0.118842	30 H	-2.890355	6.188266	-0.800303
6 H	2.890354	-6.188267	-0.800302	31 C	1.516484	0.910249	0.394313
7 C	-1.516483	-0.910248	0.394316	32 C	-1.595536	2.669991	0.149665
8 C	1.595536	-2.66999	0.149665	33 C	-0.723286	3.771952	0.159266
9 C	0.723286	-3.771952	0.159269	34 H	0.320626	3.608384	0.414423
10 H	-0.320626	-3.608383	0.414427	35 C	-1.124565	1.332481	0.387159
11 C	1.124565	-1.332481	0.387158	36 C	0.112805	0.71241	0.503291
12 C	-0.112804	-0.712409	0.503292	37 C	-1.182899	5.03146	-0.173014
13 C	1.182898	-5.03146	-0.173011	38 H	-0.5078	5.880336	-0.160024
14 H	0.507799	-5.880336	-0.16002	39 C	-2.524619	5.200429	-0.535172
15 C	2.524618	-5.200429	-0.53517	40 C	3.523694	1.811581	-0.088182
16 C	-3.523694	-1.811581	-0.088176	41 C	-2.959023	2.847636	-0.212245
17 C	2.959023	-2.847637	-0.212246	42 O	-3.842348	1.837807	-0.270989
18 O	3.842347	-1.837808	-0.270993	43 C	-3.400393	4.127532	-0.560707
19 C	3.400393	-4.127532	-0.560708	44 H	-4.441248	4.25179	-0.838839
20 H	4.441246	-4.251791	-0.838841	45 C	5.51594	0.782893	-0.519135
21 C	-5.51594	-0.782893	-0.519128	46 H	6.133819	-0.102786	-0.565803
22 H	-6.133819	0.102785	-0.565796	47 C	5.875928	2.048005	-0.807384
23 C	-5.875928	-2.048005	-0.807379	48 B	-3.560945	0.640063	0.494966
24 B	3.560945	-0.640063	0.494962	49 H	6.840419	2.403143	-1.136908
25 S	4.538887	3.136168	-0.572398	50 H	-6.840418	-2.403142	-1.136905

Table Appx-3. Cartesian coordinates of the DFT optimized geometry of **4M-anti** at the ground state calculated at the level of ω B97XD/6-31G(d).

Imaginary Freq: 0

Total Energy (Hartree): -2709.7047

Symbol	X	Y	Z	Symbol	X	Y	Z
1 S	-3.854679	3.882428	-1.286105	36 O	3.893232	1.143128	1.462164
2 O	-3.893233	-1.143128	-1.462164	37 N	2.07246	-0.000516	0.372466
3 N	-2.07246	0.000516	-0.372467	38 N	1.855933	-2.35774	0.363898
4 N	-1.855933	2.35774	-0.363899	39 N	3.943717	-1.343661	1.038201
5 N	-3.943718	1.343661	-1.0382	40 C	1.292101	1.125537	0.335879
6 C	-1.292101	-1.125537	-0.335881	41 C	-0.003949	0.718134	0.048388
7 C	0.003949	-0.718134	-0.048391	42 C	1.336512	-1.144317	0.2029
8 C	-1.336512	1.144317	-0.202901	43 C	3.110053	-2.380398	0.830163
9 C	-3.110054	2.380398	-0.830162	44 C	5.306642	-3.043194	1.746629
10 C	-5.306643	3.043195	-1.746627	45 C	5.172505	-1.718925	1.541571
11 C	-5.172506	1.718925	-1.541569	46 H	5.909959	-0.949309	1.72176
12 H	-5.90996	0.949309	-1.721758	47 C	1.925394	2.360161	0.71977
13 C	-1.925394	-2.360161	-0.719772	48 C	1.256372	3.591598	0.628626
14 C	-1.256372	-3.591598	-0.628628	49 H	0.267634	3.615552	0.176363
15 H	-0.267634	-3.615552	-0.176366	50 C	1.841036	4.743477	1.119842
16 C	-1.841037	-4.743476	-1.119844	51 H	1.325358	5.694536	1.041448
17 H	-1.325359	-5.694536	-1.041451	52 C	3.097862	4.668922	1.731295
18 C	-3.097863	-4.668922	-1.731296	53 H	3.558558	5.570056	2.12597
19 H	-3.558559	-5.570055	-2.125971	54 C	3.771293	3.462869	1.841475
20 C	-3.771294	-3.462869	-1.841475	55 H	4.745819	3.39947	2.313959
21 H	-4.74582	-3.39947	-2.313959	56 C	3.208676	2.290069	1.328443
22 C	-3.208677	-2.290069	-1.328443	57 C	4.346232	0.331208	-0.920894
23 C	-4.346231	-0.331208	0.920895	58 C	5.397709	1.245391	-1.043301
24 C	-5.397708	-1.245391	1.043302	59 H	5.694173	1.83069	-0.176024
25 H	-5.694173	-1.83069	0.176025	60 C	6.065707	1.429089	-2.252139
26 C	-6.065706	-1.42909	2.25214	61 H	6.87649	2.14953	-2.320932
27 H	-6.876488	-2.14953	2.320934	62 C	5.690774	0.693736	-3.37214
28 C	-5.690772	-0.693737	3.372141	63 H	6.206738	0.835636	-4.317718
29 H	-6.206734	-0.835638	4.31772	64 C	4.646388	-0.223533	-3.27515
30 C	-4.646385	0.223532	3.275151	65 H	4.344989	-0.799382	-4.145986
31 H	-4.344985	0.79938	4.145987	66 C	3.98738	-0.397797	-2.062817
32 C	-3.987378	0.397796	2.062817	67 H	3.171435	-1.117541	-2.009187
33 H	-3.171433	1.11754	2.009187	68 B	3.596072	0.089098	0.486341
34 B	-3.596072	-0.089098	-0.486341	69 H	-6.166132	3.570544	-2.131406
35 S	3.854677	-3.882428	1.286107	70 H	6.16613	-3.570544	2.131409

Table Appx-4. Cartesian coordinates of the DFT optimized geometry of **4M-syn(+)** at the ground state calculated at the level of ωB97XD/6-31G(d).

Imaginary Freq: 0

Total Energy (Hartree):-2709.7057

Symbol	X	Y	Z	Symbol	X	Y	Z
1 S	-4.027773	3.789075	-1.218885	36 N	2.103675	0.027055	-0.307304
2 O	-4.038169	-1.227579	-1.102583	37 N	1.911029	-2.326777	-0.475738
3 N	-2.103675	-0.027051	-0.307303	38 N	4.060295	-1.271636	-0.799372
4 N	-1.911028	2.326775	-0.475738	39 C	-0.005035	0.720865	-0.200409
5 N	-4.060296	1.271642	-0.799364	40 C	1.311356	1.146214	-0.324989
6 C	0.005036	-0.720861	-0.200411	41 C	1.363381	-1.125849	-0.315248
7 C	-1.311355	-1.14621	-0.324994	42 C	1.970598	2.397812	-0.591782
8 C	-1.36338	1.125853	-0.315245	43 C	1.27683	3.618799	-0.560766
9 C	-1.970597	-2.397806	-0.591794	44 H	0.234549	3.618858	-0.252581
10 C	-1.276829	-3.618794	-0.560782	45 C	1.902558	4.790406	-0.942219
11 H	-0.234549	-3.618855	-0.252595	46 H	1.365058	5.732056	-0.911196
12 C	-1.902556	-4.790399	-0.942242	47 C	3.230878	4.748335	-1.380987
13 H	-1.365057	-5.732025	-0.911222	48 C	3.93139	3.553933	-1.430969
14 C	-3.230875	-4.748325	-1.381013	49 H	4.960895	3.514782	-1.770854
15 C	-3.931387	-3.553923	-1.430991	50 C	3.323696	2.36059	-1.028283
16 H	-4.960891	-3.514771	-1.770878	51 C	3.215599	-2.319353	-0.772607
17 C	-3.323693	-2.360582	-1.028298	52 C	5.349078	-1.613495	-1.155246
18 C	-3.215602	2.319361	-0.77259	53 H	6.097305	-0.833817	-1.184536
19 C	-5.349085	1.613507	-1.155213	54 C	5.521208	-2.921798	-1.424417
20 H	-6.097315	0.833832	-1.184488	55 C	4.191779	0.302923	1.278353
21 C	-5.521235	2.921827	-1.424249	56 C	3.707971	-0.496168	2.323157
22 C	-4.19178	-0.302932	1.278347	57 H	2.923318	-1.225541	2.12539
23 C	-3.707979	0.496154	2.323157	58 C	4.20199	-0.379734	3.617962
24 H	-2.92333	1.225534	2.125397	59 H	3.806036	-1.009223	4.410228
25 C	-4.201999	0.379709	3.617961	60 C	5.202448	0.548869	3.898177
26 H	-3.806051	1.009196	4.410232	61 H	5.589769	0.645772	4.908658
27 C	-5.202453	-0.548901	3.898168	62 C	5.699083	1.353351	2.877478
28 H	-5.589775	-0.645813	4.908648	63 H	6.476345	2.082832	3.089251
29 C	-5.699082	-1.353379	2.877463	64 C	5.195867	1.227164	1.584279
30 H	-6.476341	-2.082866	3.08923	65 H	5.586193	1.865809	0.795371
31 C	-5.195864	-1.227181	1.584266	66 B	3.628865	0.12813	-0.222061
32 H	-5.586185	-1.865822	0.795352	67 H	6.429404	-3.423272	-1.721968
33 B	-3.628864	-0.128127	-0.222063	68 H	-6.42945	3.423316	-1.721757
34 S	4.027792	-3.789079	-1.218824	69 H	3.726039	5.665407	-1.687308
35 O	4.038172	1.227588	-1.102572	70 H	-3.726036	-5.665396	-1.687339

Table Appx-5. Cartesian coordinates of the DFT optimized geometry of **4M-syn(-)** at the ground state calculated at the level of ωB97XD/6-31G(d).

Imaginary Freq: 0

Total Energy (Hartree): -2709.7057

Symbol	X	Y	Z	Symbol	X	Y	Z
1 S	4.027773	3.789075	-1.218885	36 N	-2.103675	0.027055	-0.307304
2 O	4.038169	-1.227579	-1.102583	37 N	-1.911029	-2.326777	-0.475738
3 N	2.103675	-0.027051	-0.307303	38 N	-4.060295	-1.271636	-0.799372
4 N	1.911028	2.326775	-0.475738	39 C	0.005035	0.720865	-0.200409
5 N	4.060296	1.271642	-0.799364	40 C	-1.311356	1.146214	-0.324989
6 C	-0.005036	-0.720861	-0.200411	41 C	-1.363381	-1.125849	-0.315248
7 C	1.311355	-1.14621	-0.324994	42 C	-1.970598	2.397812	-0.591782
8 C	1.36338	1.125853	-0.315245	43 C	-1.27683	3.618799	-0.560766
9 C	1.970597	-2.397806	-0.591794	44 H	-0.234549	3.618858	-0.252581
10 C	1.276829	-3.618794	-0.560782	45 C	-1.902558	4.790406	-0.942219
11 H	0.234549	-3.618855	-0.252595	46 H	-1.365058	5.732056	-0.911196
12 C	1.902556	-4.790399	-0.942242	47 C	-3.230878	4.748335	-1.380987
13 H	1.365057	-5.732025	-0.911222	48 C	-3.93139	3.553933	-1.430969
14 C	3.230875	-4.748325	-1.381013	49 H	-4.960895	3.514782	-1.770854
15 C	3.931387	-3.553923	-1.430991	50 C	-3.323696	2.36059	-1.028283
16 H	4.960891	-3.514771	-1.770878	51 C	-3.215599	-2.319353	-0.772607
17 C	3.323693	-2.360582	-1.028298	52 C	-5.349078	-1.613495	-1.155246
18 C	3.215602	2.319361	-0.77259	53 H	-6.097305	-0.833817	-1.184536
19 C	5.349085	1.613507	-1.155213	54 C	-5.521208	-2.921798	-1.424417
20 H	6.097315	0.833832	-1.184488	55 C	-4.191779	0.302923	1.278353
21 C	5.521235	2.921827	-1.424249	56 C	-3.707971	-0.496168	2.323157
22 C	4.19178	-0.302932	1.278347	57 H	-2.923318	-1.225541	2.12539
23 C	3.707979	0.496154	2.323157	58 C	-4.20199	-0.379734	3.617962
24 H	2.92333	1.225534	2.125397	59 H	-3.806036	-1.009223	4.410228
25 C	4.201999	0.379709	3.617961	60 C	-5.202448	0.548869	3.898177
26 H	3.806051	1.009196	4.410232	61 H	-5.589769	0.645772	4.908658
27 C	5.202453	-0.548901	3.898168	62 C	-5.699083	1.353351	2.877478
28 H	5.589775	-0.645813	4.908648	63 H	-6.476345	2.082832	3.089251
29 C	5.699082	-1.353379	2.877463	64 C	-5.195867	1.227164	1.584279
30 H	6.476341	-2.082866	3.08923	65 H	-5.586193	1.865809	0.795371
31 C	5.195864	-1.227181	1.584266	66 B	-3.628865	0.12813	-0.222061
32 H	5.586185	-1.865822	0.795352	67 H	-6.429404	-3.423272	-1.721968
33 B	3.628864	-0.128127	-0.222063	68 H	6.42945	3.423316	-1.721757
34 S	-4.027792	-3.789079	-1.218824	69 H	-3.726039	5.665407	-1.687308
35 O	-4.038172	1.227588	-1.102572	70 H	3.726036	-5.665396	-1.687339

Table Appx-6. Cartesian coordinates of the DFT optimized geometry of **5M** at the ground state calculated at the level of ω B97XD/6-31G(d).

Imaginary Freq: 0

Total Energy (Hartree): -2496.7554

Symbol	X	Y	Z	Symbol	X	Y	Z
1 C	0.661081	-0.259476	-0.022884	27 C	-3.651949	0.282124	-0.631897
2 C	-0.661081	0.259476	-0.022884	28 S	2.327825	-5.110431	-0.388833
3 C	-0.54185	1.682539	0.013315	29 C	1.049752	-6.28851	-0.468871
4 N	0.812122	1.975702	0.082116	30 C	-0.152711	-5.697266	-0.330459
5 C	1.552296	0.792053	0.056697	31 N	-0.089433	-4.328172	-0.158729
6 C	0.54185	-1.682539	0.013315	32 S	-2.327825	5.110431	-0.388833
7 N	-0.812122	-1.975702	0.082116	33 C	-1.049752	6.28851	-0.468871
8 C	-1.552296	-0.792053	0.056697	34 C	0.152711	5.697266	-0.330459
9 C	1.156511	-3.847033	-0.169561	35 F	-1.751162	-3.758476	1.454834
10 C	-1.156511	3.847033	-0.169561	36 F	-2.327825	-3.690025	-0.762613
11 N	0.089433	4.328172	-0.158729	37 F	2.327825	3.690025	-0.762613
12 N	-1.517823	2.569727	-0.071603	38 F	1.751162	3.758476	1.454834
13 B	1.343724	3.437998	0.164236	39 H	3.301322	2.344751	1.502241
14 N	1.517823	-2.569727	-0.071603	40 H	5.748101	2.093828	1.583667
15 B	-1.343724	-3.437998	0.164236	41 H	5.516424	-1.188088	-1.17795
16 C	3.013447	0.720118	0.111894	42 H	3.061466	-0.955313	-1.24195
17 C	-3.013447	-0.720118	0.111894	43 H	-3.301322	-2.344751	1.502241
18 C	3.782391	1.576075	0.911483	44 H	-5.748101	-2.093828	1.583667
19 C	5.16193	1.429593	0.956376	45 H	-5.516424	1.188088	-1.17795
20 C	5.791494	0.440285	0.205317	46 H	-3.061466	0.955313	-1.24195
21 C	5.033024	-0.41433	-0.589709	47 H	1.258412	-7.337904	-0.611288
22 C	3.651949	-0.282124	-0.631897	48 H	-1.123204	-6.172376	-0.33887
23 C	-3.782391	-1.576075	0.911483	49 H	-1.258412	7.337904	-0.611288
24 C	-5.16193	-1.429593	0.956376	50 H	1.123204	6.172376	-0.33887
25 C	-5.791494	-0.440285	0.205317	51 H	6.871762	0.334396	0.24162
26 C	-5.033024	0.41433	-0.589709	52 H	-6.871762	-0.334396	0.24162

Table Appx-7. Cartesian coordinates of the DFT optimized geometry of **6M** at the ground state calculated at the level of ωB97XD/6-31G(d).

Imaginary Freq: 0

Total Energy (Hartree): -3138.2809

Symbol	X	Y	Z	Symbol	X	Y	Z		
1	S	-4.948634	2.698388	0.028343	24	C	5.712274	-0.270135	-0.170583
2	C	-3.763775	1.427619	0.007136	25	C	6.220691	-1.5171	-0.150204
3	N	-4.334003	0.223204	0.089387	26	B	3.521809	1.118564	-0.042585
4	C	-5.71243	0.270119	0.170892	27	F	3.799995	1.850394	-1.17627
5	C	-6.220857	1.517083	0.150684	28	F	3.885384	1.793706	1.111566
6	B	-3.521974	-1.118551	0.04248	29	N	2.46222	-1.688473	0.06934
7	F	-3.800072	-1.850527	1.176093	30	N	2.02795	0.679388	0.010607
8	F	-3.885684	-1.793514	-1.111733	31	C	1.638735	-0.651191	0.041456
9	N	-2.462416	1.688485	-0.069327	32	C	0.902667	1.501186	-0.029295
10	N	-2.028109	-0.679379	-0.010798	33	C	-0.215656	0.675455	-0.028473
11	C	-1.638907	0.651214	-0.041599	34	C	0.916065	2.944489	-0.080961
12	C	-0.902795	-1.501156	0.029051	35	C	-0.138743	3.694964	-0.566227
13	C	0.215492	-0.675401	0.028246	36	H	-1.043151	3.243494	-0.951964
14	C	-0.915984	-2.944461	0.080797	37	C	0.080009	5.086929	-0.482673
15	C	0.139054	-3.694673	0.565972	38	H	-0.627391	5.833395	-0.822124
16	H	1.043403	-3.242965	0.951578	39	C	1.290969	5.383163	0.081299
17	C	-0.079389	-5.086692	0.482538	40	S	2.184463	3.9886	0.50357
18	H	0.628211	-5.832975	0.821974	41	H	-1.70732	-6.362945	-0.274253
19	C	-1.290335	-5.383234	-0.081301	42	H	1.708158	6.362767	0.274351
20	S	-2.184137	-3.988901	-0.503685	43	H	-7.25853	1.809537	0.202247
21	S	4.948447	-2.698389	-0.027931	44	H	-6.258071	-0.659928	0.241173
22	C	3.76359	-1.427614	-0.00698	45	H	6.257928	0.659903	-0.240877
23	N	4.333837	-0.223206	-0.089252	46	H	7.258369	-1.809563	-0.201613

Table Appx-8. Cartesian coordinates of the DFT optimized geometry of **4M-anti** at the excited state (S_1) calculated at the level of ω B97XD/6-31G(d).

Total Energy (Hartree): -2709.6238

Symbol	X	Y	Z	Symbol	X	Y	Z		
1	S	-3.873	3.864	-1.324	36	O	3.896	1.175	1.447
2	O	-3.896	-1.175	-1.447	37	N	2.087	0.019	0.351
3	N	-2.087	-0.019	-0.351	38	N	1.868	-2.34	0.401
4	N	-1.868	2.34	-0.401	39	N	3.954	-1.317	1.058
5	N	-3.954	1.317	-1.058	40	C	1.319	1.139	0.31
6	C	-1.319	-1.139	-0.31	41	C	-0.007	0.706	0.037
7	C	0.007	-0.706	-0.037	42	C	1.352	-1.126	0.204
8	C	-1.352	1.126	-0.204	43	C	3.118	-2.364	0.862
9	C	-3.118	2.364	-0.862	44	C	5.322	-3.013	1.767
10	C	-5.322	3.013	-1.767	45	C	5.183	-1.689	1.552
11	C	-5.183	1.689	-1.552	46	H	5.924	-0.92	1.721
12	H	-5.924	0.92	-1.721	47	C	1.922	2.374	0.696
13	C	-1.922	-2.374	-0.696	48	C	1.238	3.602	0.613
14	C	-1.238	-3.602	-0.613	49	H	0.251	3.618	0.155
15	H	-0.251	-3.618	-0.155	50	C	1.808	4.754	1.119
16	C	-1.808	-4.754	-1.119	51	H	1.281	5.699	1.048
17	H	-1.281	-5.699	-1.048	52	C	3.065	4.692	1.733
18	C	-3.065	-4.692	-1.733	53	H	3.513	5.596	2.136
19	H	-3.513	-5.596	-2.136	54	C	3.755	3.492	1.836
20	C	-3.755	-3.492	-1.836	55	H	4.727	3.438	2.314
21	H	-4.727	-3.438	-2.314	56	C	3.209	2.319	1.314
22	C	-3.209	-2.319	-1.314	57	C	4.371	0.328	-0.922
23	C	-4.371	-0.328	0.922	58	C	5.419	1.246	-1.049
24	C	-5.419	-1.246	1.049	59	H	5.703	1.848	-0.188
25	H	-5.703	-1.848	0.188	60	C	6.097	1.414	-2.254
26	C	-6.097	-1.414	2.254	61	H	6.905	2.138	-2.327
27	H	-6.905	-2.138	2.327	62	C	5.738	0.658	-3.365
28	C	-5.738	-0.658	3.365	63	H	6.262	0.788	-4.308
29	H	-6.262	-0.788	4.308	64	C	4.697	-0.263	-3.264
30	C	-4.697	0.263	3.264	65	H	4.408	-0.855	-4.128
31	H	-4.408	0.855	4.128	66	C	4.028	-0.422	-2.055
32	C	-4.028	0.422	2.055	67	H	3.215	-1.145	-1.997
33	H	-3.215	1.145	1.997	68	B	3.61	0.106	0.481
34	B	-3.61	-0.106	-0.481	69	H	-6.187	3.533	-2.152
35	S	3.873	-3.864	1.324	70	H	6.187	-3.533	2.152

Table Appx-9. Cartesian coordinates of the DFT optimized geometry of **4M-sym(+)** at the excited state (S_1) calculated at the level of ω B97XD/6-31G(d).

Total Energy (Hartree): -2709.6241

Symbol	X	Y	Z	Symbol	X	Y	Z
1 S	-4.07174	3.791499	-1.177274	36 N	2.11516	0.041331	-0.342275
2 O	-4.063408	-1.246136	-1.08873	37 N	1.93104	-2.314433	-0.525487
3 N	-2.11516	-0.041328	-0.34227	38 N	4.084355	-1.257763	-0.796129
4 N	-1.931042	2.314437	-0.525461	39 C	-0.008494	0.707504	-0.292344
5 N	-4.084357	1.25777	-0.796108	40 C	1.338415	1.155539	-0.372735
6 C	0.008493	-0.707501	-0.29235	41 C	1.377716	-1.110939	-0.365018
7 C	-1.338416	-1.155536	-0.372742	42 C	1.980261	2.405694	-0.622823
8 C	-1.377717	1.110942	-0.365005	43 C	1.277849	3.626251	-0.615713
9 C	-1.980263	-2.405688	-0.62284	44 H	0.22723	3.621622	-0.334387
10 C	-1.277851	-3.626245	-0.615742	45 C	1.907654	4.797632	-0.988246
11 H	-0.22723	-3.621619	-0.334419	46 H	1.36346	5.736222	-0.976959
12 C	-1.907656	-4.797623	-0.988284	47 C	3.248234	4.764593	-1.393183
13 H	-1.363462	-5.736213	-0.977007	48 C	3.958488	3.573431	-1.421201
14 C	-3.248237	-4.76458	-1.393218	49 H	4.995628	3.540071	-1.737957
15 C	-3.958491	-3.573418	-1.421223	50 C	3.349616	2.379636	-1.029359
16 H	-4.995632	-3.540056	-1.737976	51 C	3.23791	-2.315224	-0.779906
17 C	-3.349618	-2.379627	-1.029372	52 C	5.380072	-1.604576	-1.103171
18 C	-3.237912	2.315231	-0.779878	53 H	6.130807	-0.826588	-1.119803
19 C	-5.380075	1.604585	-1.103144	54 C	5.564709	-2.91844	-1.347855
20 H	-6.13081	0.826598	-1.119781	55 C	4.164448	0.305825	1.290581
21 C	-5.564712	2.918452	-1.347817	56 C	3.650678	-0.489894	2.323565
22 C	-4.164445	-0.305836	1.290589	57 H	2.864306	-1.212194	2.107618
23 C	-3.650671	0.489872	2.323579	58 C	4.116302	-0.377489	3.629162
24 H	-2.864299	1.212175	2.107635	59 H	3.697133	-1.003614	4.412156
25 C	-4.116292	0.377456	3.629175	60 C	5.118336	0.542318	3.932181
26 H	-3.697121	1.003574	4.412174	61 H	5.483719	0.635592	4.951149
27 C	-5.118326	-0.542353	3.932189	62 C	5.644679	1.3427	2.923217
28 H	-5.483706	-0.635636	4.951157	63 H	6.423026	2.06565	3.152735
29 C	-5.644672	-1.342725	2.923219	64 C	5.169382	1.221481	1.618972
30 H	-6.423018	-2.065678	3.152733	65 H	5.581938	1.857713	0.839419
31 C	-5.169378	-1.221495	1.618974	66 B	3.638436	0.138145	-0.223493
32 H	-5.581937	-1.85772	0.839417	67 H	6.484771	-3.418579	-1.609621
33 B	-3.638437	-0.138143	-0.223486	68 H	-6.484775	3.418593	-1.609577
34 S	4.071736	-3.791489	-1.177318	69 H	3.7441	5.684336	-1.689965
35 O	4.063405	1.246146	-1.088729	70 H	-3.744104	-5.684321	-1.690007